Geological Survey of Finland

2024

Geological and mineralogical investigations of high-quality flake graphite occurrences in Finland

Thair Al-Ani, Timo Ahtola, Janne Kuusela, Seppo Leinonen and Hanna Leväniemi

GTK Open File Research Report 13/2024

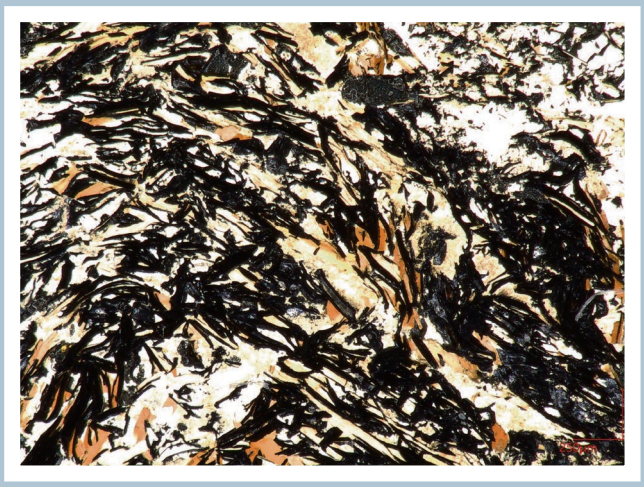

GTK

GEOLOGICAL SURVEY OF FINLAND

Open File Research Report 13/2024

Thair Al-Ani, Timo Ahtola, Janne Kuusela, Seppo Leinonen and Hanna Leväniemi

Geological and mineralogical investigations of high-quality flake graphite occurrences in Finland

Unless otherwise indicated, the figures have been prepared by the authors of the report.

Front cover: The graphite-bearing schist and gneiss, the graphite flakes show strongly foliated schist and high-purity graphite powder.
Photo: Thair Al-Ani, GTK.

Layout: Elvi Turtiainen Oy

Espoo 2024

Al-Ani, T., Ahtola, T., Kuusela, J., Leinonen, S. & Leväniemi, H. 2024. Geological and mineralogical investigations of high-quality flake graphite occurrences in Finland. *Geological Survey of Finland, Open File Research Report 13/2024*, 39 pages, 25 figures and 7 tables.

This study presents mineralogical and geochemical results from recent graphite exploration at three potentially important graphite occurrences in Rautalampi–Käpysuo, Raisjoki–Emas and Joutsijärvi–Kuusivaara. These flake graphite targets represent a retrograde metamorphic terrain of Finland and are mainly hosted by black schist, mica-quartz gneiss and rarely by amphibolite rocks.

Graphite flakes in the studied samples ranged in size from 50 to 1600 µm in length, with Käpysuo and Joutsijärvi having both medium flakes (150–400 µm) and coarse flakes, while graphite flakes at Raisjoki and Emas were mostly fine (<150 µm). The average content of graphitic carbon (Cg) ranged from 5.20–38.0 wt% (avg. 12.0 wt% C), 4.14–11.50 wt% (avg. 6.85 wt% C) and 4.9–32.10 (avg. 9.90 wt% C) at Käpysuo, Raisjoki and Joutsijärvi, respectively.

Beneficiation tests were performed on two composite drill core samples from Käpysuo and Raisjoki to produce high-purity graphite concentrates that are particularly suitable for lithium-ion batteries. After multi-stage grinding and flotation processes, the best grade of the final concentrate contained 85% fixed carbon at 88% recovery for the Käpysuo graphite sample and 89% fixed carbon at 66% recovery for the Raisjoki graphite sample. Purification by alkaline roasting and acid leaching increased the fixed carbon content to 99.4% for the Käpysuo sample with fine particle sizes of <50 µm and >99.0% C for the Raisjoki sample with fine particle sizes of <20 µm. These results demonstrate that the purity of the studied graphite concentrates can be increased to obtain high-grade graphite required for lithium-ion batteries.

Keywords: flake graphite, flotation, purification, acid leaching, alkaline roasting, battery minerals, Rautalampi, Raisjoki, Joutsijärvi

Thair Al-Ani
Geological Survey of Finland
P.O. Box 96
FI-02151 Espoo, Finland

E-mail: thair.alani@gtk.fi

CONTENTS

1 INTRODUCTION

Finland has a good potential for new flake graphite deposits due to the lithologies of the bedrock and a suitable metamorphic grade. However, it is rare to find economically interesting deposits. More than 50 flake graphite occurrences were registered in Finland during the years 1760–1947, of which >30 have been mined (Fig. 1a). The total output of these mines has been approximately 14 000 tons. The largest of the past graphite mines were Kärpäla, which was mined from 1850 to 1947, producing about 600 of graphite ore with an average content of 40% C, and Soukko, which was mined in 1917, producing 500 tons of graphite ore with an average content of 50% (Puustinen 2003).

The Geological Survey of Finland has conducted extensive exploratory studies on graphite in recent years on the basis that the qualities of the bedrock and metamorphic grade in Finland are suitable for economically potential graphite deposits. According to historical data, in the southeastern region, there are several small flake graphite occurrences, such as Pertunmaa (5–10 wt% C) and Kärpälä (40 wt% C) at Mäntyharju, but due to their small size, they currently lack commercial value. Showings of flake graphite are also known in the Lapland granulite belt (Isomaa 1991, 1993) and the Joutsijärvi area near Kemijärvi (Pankka 1999). The amorphous graphite deposits in Juuka, Kiihtelysvaara (29 wt% C) and Kolari contain several million tons of fine-grained graphite. However, flotation tests yielded carbon contents too low for these deposits to be economically viable, especially concerning high-tech products (Sarapää 1988, Sarapää & Kukkonen 1984).

Currently, the Aitolampi deposit in Heinävesi is the most advanced graphite exploration project in Finland, developed by Grafintec Oy, Beowulf Mining's Finnish subsidiary. It serves as an example of a recent prospect, with indicated and inferred resources of 26.7 Mt at a grade of 4.8% TGC, 4.7% S, 2.81 t/m3 density, and 1.275 kt contained graphite.

Graphite-bearing rocks are usually characterized by schistose foliation and gneiss rocks, and less commonly by amphibolite. These rocks are mostly associated with high-grade metamorphic rocks (amphibolite/granulite facies), where organic carbon deposited within sediment has transforms into crystalline graphite under pressures typically exceeding ≥5 Kbar and temperatures around 650 to 700 °C (Fig. 1b). Graphite flakes found in Finnish rocks exhibit a range of sizes, with most being coarse-flaked findings. Fine flakes (<150 µm) are observed in Talvivaara and Raisjoki graphite, while occurrences such as Rautalampi–Käypysuo and Koivuniemi graphite boast medium flakes (150–400 µm) and coarse flakes (400–1600 µm), as documented by Al-Ani et al. (2016, 2018, 2020, 2022) and Kuusela et al. (2021, 2022).

In this report, we provide a summary of previous graphite exploration, airborne geophysics and ongoing graphite exploration projects developing the future battery minerals potential and industry. In each chapter, our descriptions focus on what is considered relevant to graphite mineralisations. Further petrographic and mineralogical studies were carried out on the unknown graphite occurrences in Finland. Additionally, purification techniques were employed to produce high-quality graphite with an exceptionally low concentration of impurities, meeting the requirements for lithium-ion battery anode applications.

2 CHARACTERISTICS OF GRAPHITE MINERALIZATION

Flake graphite is predominantly found in high-grade metamorphic rocks, where the transformation of organic carbon deposited in sediment occurs under pressures exceeding 5 kbar and temperatures ranging from 650 to 700 °C (Fig. 2). Natural graphite deposits manifest in three primary geological contexts: flake graphite dispersed in metamorphosed sedimentary rocks such as gneiss or schist, amorphous graphite resulting from the metamorphism of coal or carbon-rich sediments, and vein/lump graphite filling fractures in granitic country rocks. The term 'amorphous graphite' is commercially used and somewhat misleading, as all graphite inherently possesses a crystalline structure, albeit with varying degrees of crystallinity. The trade's reference to fine crystalline flake as 'amorphous' can create confusion when assessing graphite production and markets. Additionally, graphite can be synthetically manufactured from carbon-bearing raw materials such as petroleum coke, with synthetic graphite commanding a significantly higher price than its natural counterpart. Natural graphite products often contain traces of mineral impurities related to the origin of the raw material, including silicate and sulphide minerals such as quartz, mica or pyrite in the case of flake graphite.

In lithium-ion batteries, graphite plays a crucial role as the material in the negative electrode, while intercalated lithium compounds are used in the positive electrode. Battery-grade graphite, essential for this application, can be derived from either natural or synthetic sources. Among natural graphite varieties, only flake graphite is suitable for battery production and is found in high-grade metamorphic rocks such as marbles, schists and gneisses, originating from either fluid deposition or graphitization. To meet the requirements of battery-grade graphite, high purity (>99.95 wt% C) spherical particles with sizes ranging from 10 to 25 µm are necessary for effective performance.

The production of spherical graphite involves processes such as micronizing, rounding and purifying techniques. Additionally, spherical graphite can also be produced from synthetic graphite (European Commission 2018).

Based on investigations by GTK, graphite mineralization is described as occurring in multiple thin layers and lenses, with layers being a few metres thick and lenses being small but having a high carbon content. The quality of the graphite is reported to be good, with graphite schist appearing as medium to coarse-grained flake graphite at most localities, such as Rautalampi, Käypysuo and Joutsijärvi–Kuusivaara, while fine-grained flake graphite is recognized at Raisjoki and Talvivaara.

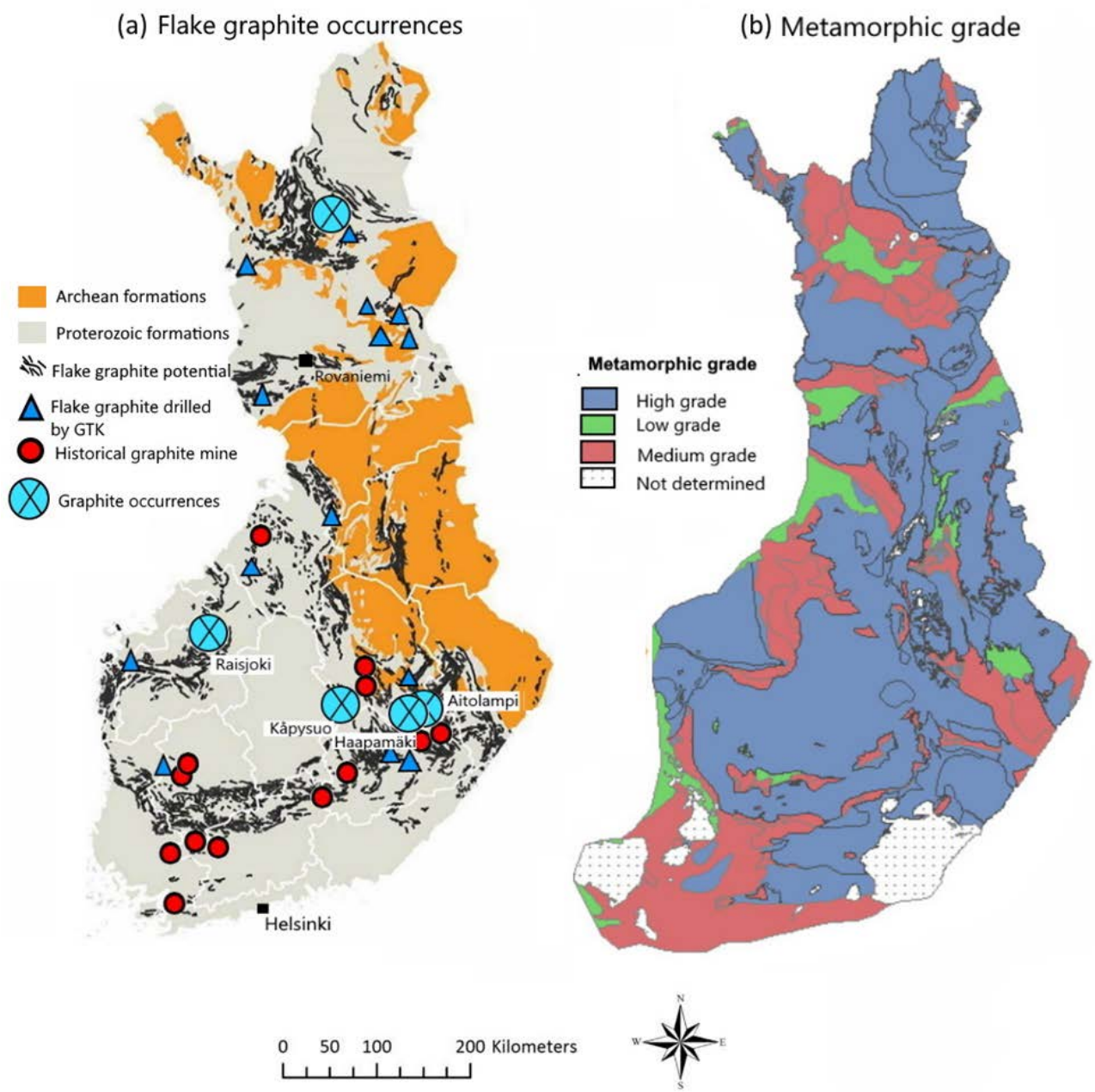

Fig. 1. a) The locations of black schists (black lines) and graphite occurrences in Finland. b) Low-, medium- and high-grade metamorphic areas.

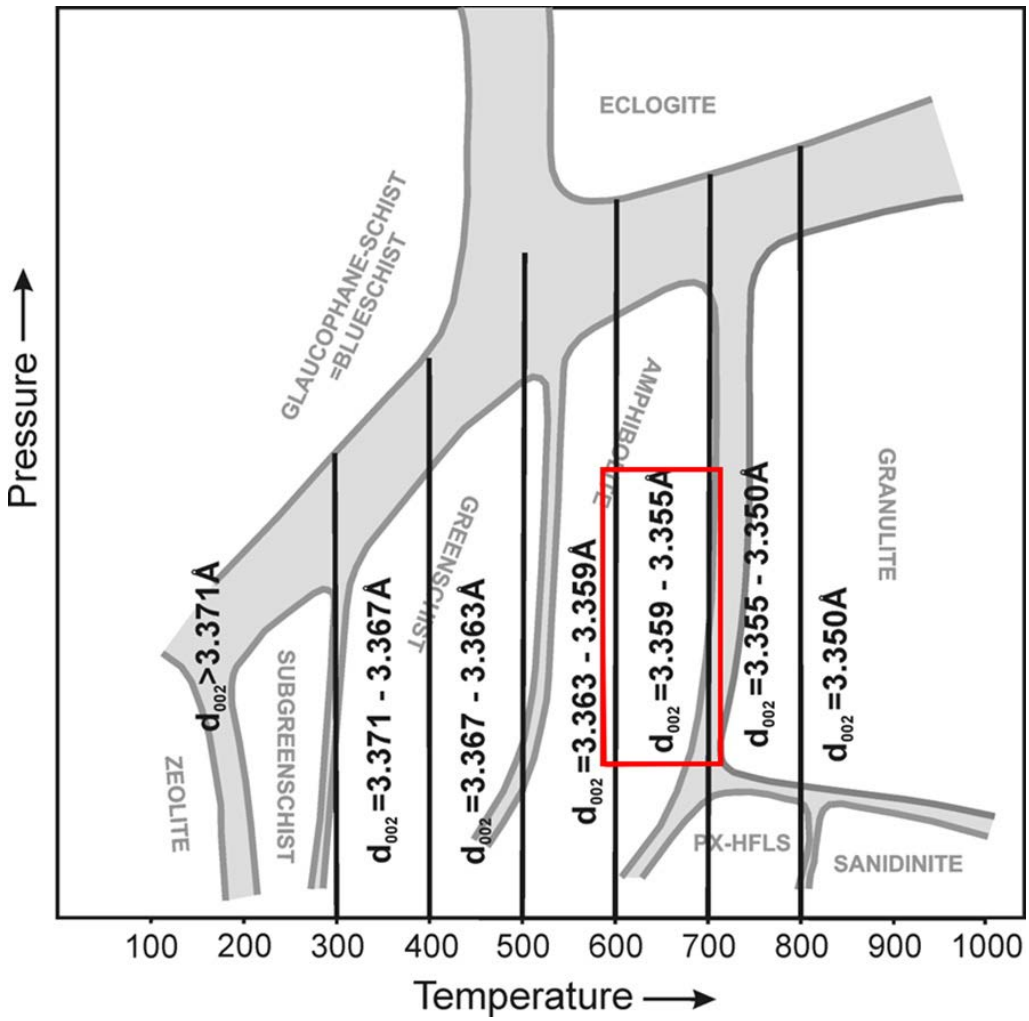

Fig. 2. P–T diagram showing the relative position of the facies in the P–T field. The studied samples (outlined in red) fall in the field of the amphibolite facies (modified after Smulikowski et al. 2007).

3 PREVIOUS AND ON-GOING GRAPHITE INVESTIGATIONS

Finland has had many historical graphite sites of interest that may still contain valuable raw materials. Many of these historical targets produced graphite for dry lubricants and were decommissioned before some technologies were developed to use the graphite as an anode material in lithium-ion batteries. Many historical graphite sites of interest were discovered by GTK and other mining companies, and these may still have economic potential for graphite (Table 1).

Table 1. Summary of some graphite prospects in Finland discovered by GTK and mining companies (modified after Puustinen 2003).

Project area	Type	Size km^2	Drill holes	Comments
Kolari	Claim Reservation	13.8	8 diamond drill holes (1918-1985) Rautaruukki Oy, Kiiruna AB, GTK	Host rock: graphitic schist, Grade 15-30 % Cg & 3 Mt Indicated. Coord. 234721 E, 6719540 N
	Ore Prospecting Licence	5.5		
Tunturi	Claim Reservation	99.12	32 diamond drill holes (1996-1997) GTK	Flaky graphite reported. Coord. 274937 E, 6538436 N
Polvela	Ore Prospecting Licence	9.2	4 diamond drill holes (1983) GTK	Hole R303 – 29m @ 18% C from 13m depth Coord. 295847 E, 640234 N
Viistola/ Hyypiä	Ore Prospecting Licence	1.36	13 diamond drill holes (1972-1983) GTK	Hole R430 – 14.6m @ 31.8% C from 48.5m Coord. 01747 E, 6225510 N
Aitoo	Claim Reservation	187.11	15 diamond drill holes (1983-1992) GTK, Outokumpu Oy	Hole R336 – 7.6m @ 34.8% C from 7.4m. Hole R331 – 99.55m @ 12.1% C from 5m
Misi	Claim Reservation	170.56	75 diamond drill holes (1955–2006) GTK, Rautaruukki Oy, Lapin Malmi Oy	Competing application
Aitolampi	Ore Prospecting Licence	1.20	16 diamond drill holes (2017–2018), Beowulf mining	Indicated + Inferred graphite deposit of 26.7 Mt @ 4.1% TGC

The historic Finnish graphite deposits have previously been described by Laitakari (1925), Sarapää & Kukkonen (1984) and Sarapää (1988). Laitakari (1925) listed ~150 graphite occurrences and concluded that graphite is regularly associated with paragenesis, mica gneisses and metamorphosed limestone. Only small, lenticular graphite flake deposits from Svecofennian metasediments have been mined. Aurola (1965) listed 15 small deposits with carbon contents of ≥10%, of which only 4 contain ≥30% carbon: Rääpysjärvi (Kuopio) 60.8%, Soukko (Vammala) 49.6%, Kärpälä (Mäntyharju) 39.0% and Laivonsaari (Kuopio) 32.6%. In the 1970s, GTK and Rautaruukki searched for graphite in several exploration targets. Rautaruukki's work was conducted in Kolari and Misi, and GTK's studies were in Inari and Kemijärvi's Joutsijärvi. The average graphite contents were 8.9% C_{gr} in the Kolari graphite prospect and 15–30% C_{gr} in Juurakkajärvi and Saarenputaa. Based on a combination of geophysical anomalies and a diamond drillhole, an exploration target was identified with an estimated three million tons, ranging from 15–30 % C_{gr} to a vertical depth of 50 metres (Mattila 1978, Sarapää & Kukkonen 1984). Later investigations (Sarapää 1988) partially focused on the potential energy source from graphite-rich schists, of which the best evaluated deposits are at Hyypiä, Kiihtelysvaar in Joensuu (11 Mt rock with 28.6 wt% C, 2.3 wt% S) and Polvela, Juuka (2.5 Mt with 18 wt% C, 1.5–2 wt% S), both in North Karelia. Volumetrically, most graphite of the previously explored deposits in Finland occurs in the marine uppermost Jatulian sedimentary rocks and in the Kalevian black schists (Sarapää 1988, Arkimaa et al. 2000). Flake-type graphite

targets have been explored by GTK in Jahtisneva (Meijärvi) and Kaukkala (Pälkäne). Drill cores from the Merijäri deposit have a graphitic carbon content of 10–25 wt% C_{gr}, being at highest 40–50 wt%, and a very low sulphur content of ≈1 wt% S. The grain size varies from coarse flakes (<1000 µm) to fine flakes (Aurola 1965), while drill core samples from Pälkäne contain on average 12 wt% C_{gr} and 7 wt% S. The maximum carbon content was 48 wt%, with 6 wt% sulphur (Alviola & Nurmela 1994). The Kaukkala graphite is coarse grained, with the longest flakes being 1000 µm and the average length being approximately 400 µm (Al-Ani et al. 2019).

Otanmäki Oy has been drilled in Misi on the east side of Venejärvi: a 10–25-m-thick graphite shale layer containing 23.8–27.7 C_{gr} and 1.8–6.5% S was identified in the drillings. According to Nuutilainen (1968), there are also other conductors caused by graphite in the area. The best intersections of the graphite in Venejärvi and Tervakanka in Misi were 30.7% C_{gr} @ depth 33.4 m in borehole R3 and 29.5% C_{gr} @ depth 42.00–53.00 m in borehole R1. In the above-mentioned sites, the graphite is not flake-like but fine-grained mass-like. The best intersection was 23.55 m @ 10.6% C_{gr} in the Koivuniemi target.

In early 2012, Cullen Resources Limited (Cullen) lodged three ore prospecting license applications (exploration license equivalents) and four claim reservation applications over six graphite prospects in the name of its wholly owned, Finnish-registered subsidiary company. The historical work carried out by GTK was aimed at the potential of graphite as a fuel source. Cullen may now begin work on these prospects during the application stage of the licenses and the life of the claim reservations (two years) by examining the drill cores in Finland, resampling and analysing parts of the core, and re-assessing the drill and geophysical databases, as described on the following website: http://cullenresources.com.au.

Currently, there is no mine production of graphite in Finland. The Aitolampi deposit in Heinävesi is the most advanced exploration project for graphite in the country. The mineral resources (indicated + inferred) of 19.3 Mt have been estimated to contain 878 000 t graphite. Grafintec Oy (formerly Fennoscandian Resources), a Finnish subsidiary of the British company Beowulf Ltd, is carrying out characterization tests on the concentrates to determine the potential industrial applications of the graphite (Beowulf Mining 2022). The project is located within the scenic Finnish landscape of the Saimaa Lake region, a popular summer holiday destination with many vacation homes, and is opposed by local communities (Leino & Miettinen 2020, Eerola 2022). Previous studies have shown that graphite occurrences of interest are present in the Fennoscandian Shield with high-quality and high-grade metamorphism (Palosaari et al. 2016, Palosaari 2021).

GTK identified multiple potential areas for graphite exploration in Finland for use in energy production during the 1980s, including graphite occurrences at Joutsijärvi, Venejärvi, Jaurujoki, Haapamäki, Rytijänkä and Tervola (Al-Ani & Sarapää 2016, Sarapää & Kukkonen 1984), which were later explored for flake graphite ores and for flake graphite production (Al-Ani et al. 2016).

The EC included graphite on the list of strategic and critical raw materials in 2014. Therefore, GTK has accumulated not only geological but also geophysical data, along with re-logging and analysis of drill cores from known graphite prospects to discover new flake graphite occurrences in Finland. In addition to a geophysical survey and drill programme, the drill core research material was complemented by boulder and outcrop samples taken from the entire country.

4 PURPOSE OF THE STUDY

In this study, the mineralogy and the geochemical and beneficiation process of graphite flakes were investigated using new analytical methods, including digital microscopy| EM elemental analysis, X-ray diffraction analysis (XRD), Raman spectroscopy and scanning electron microscopy (SEM), geochemical analysis, and beneficiation processes (flotation & purification) that would obtain high-grade graphite required for lithium-ion battery production. The aims were to increase knowledge of known and previously unknown graphite occurrences in Finland and to make the data

available for further investigations by researchers or prospecting companies. The mapping, exploration, drilling and characterization of several flake graphite occurrences in Finland were performed by GTK (2016–2022). This study relates to several GTK projects on graphite exploration, e.g., the Green Minerals Project (2018–2020), the Battery Mineral Project (2016–2019 & 2019–2022) and BatCircle 1.0 & 2.0 (2019–2020, 2021–2024), in which the mineral potential evaluation was conducted with an emphasis on flake graphite, cobalt and lithium. In this report, we present the data and results from recent flake graphite exploration of four potentially important graphite occurrences in Rautalampi–Käpysuo (31 drill holes), Raisjoki–Emas (4 drill holes) and Joutsijärvi–Kuusivaara (7 drill holes). We also provide a brief review of the earlier work conducted by GTK in the studied areas. In each chapter, we limit our descriptions to what is regarded relevant to graphite mineralisations.

5 EXPLORATION METHODS

The methods used in this work were chosen according to their suitability for analysing graphite flakes. Due to the high conductivity of graphite, electromagnetic (EM) and magnetic susceptibility ground surveying were used to evaluate the flaky graphite occurrences in Finland. Graphite displays characteristic features in X-ray diffraction and Raman spectroscopy analysis, which are rapid and non-destructive analytical methods. Scanning electron microscopy was used to analyse the characteristics of the liberated graphite flakes and to identify unidentified minerals and impurities within the graphite concentrate. Beneficiation studies were performed to produce high-purity graphite concentrate (flotation separation and purification techniques). The peak metamorphic temperatures were obtained using Raman spectroscopy of carbonaceous material (RSCM) geothermometry, together with classic geothermometry and P–T pseudosections.

5.1 Geophysical methods

During 1972–2007, GTK conducted low high-resolution, low-altitude aeromagnetic anomaly greyscale and colour mapping (Fig. 3) covering the whole of Finland (Hautaniemi et al. 2005). The ground-sents was applied in graphite research projects at GTK to evaluate the flaky graphite occurrences in Finland.

Both selected techniques, ground electromagnetic (EM) and electrical resistivity tomography (ERT) methods, were applied to supply information on Käypysuo flake graphite. Four-frequency MaxMin EM measurements (using a 100–200 m coil spacing) and low-induction EM minislingram GEM-2 (Geophex Ltd., Won et al. 1996) were applied at six profiles and ERT at two (600 m spear and 121 electrodes). MaxMin (at 800 Hz frequency) provided information on deeper (≈ 40–60 m) conductors compared to GEM-2. The results were compared with the slingram EM anomalies of the previous study (Fig. 4a). Variable and partly deep overburden (10–50 m) and strong magnetic anomalies in the middle of the site complicate the interpretation of EM data. A significant and almost impossible challenge is to distinguish whether the conductor is flake graphite schist or black shale. Testing of the frequency electromagnetic (FrEM) method was also carried out, which involves conducting measurements within specific frequency ranges. FrEM surveys with five frequencies (116–8929 Hz) located the conductive zones in the same positions as the slingram method. With the device used in this study, it was possible to use up to 41 frequencies, ranging from 100 to 10 000 Hz, and also to perform a layer model interpretation. At Raisjoki, a total of 48 profiles were collected every 50 m using a slingram PROMIS FDEM system with 0.8 kHz, 3.5 kHz and 14 kHz in-phase components. Low frequencies present the strongest electrical conductivity anomalies and have better depth penetration compared to the high-frequency in-phase components. The frequency domain method measures the electrical conductivity of the subsurface with real (Re) components of the secondary magnetic field (Fig. 4b).

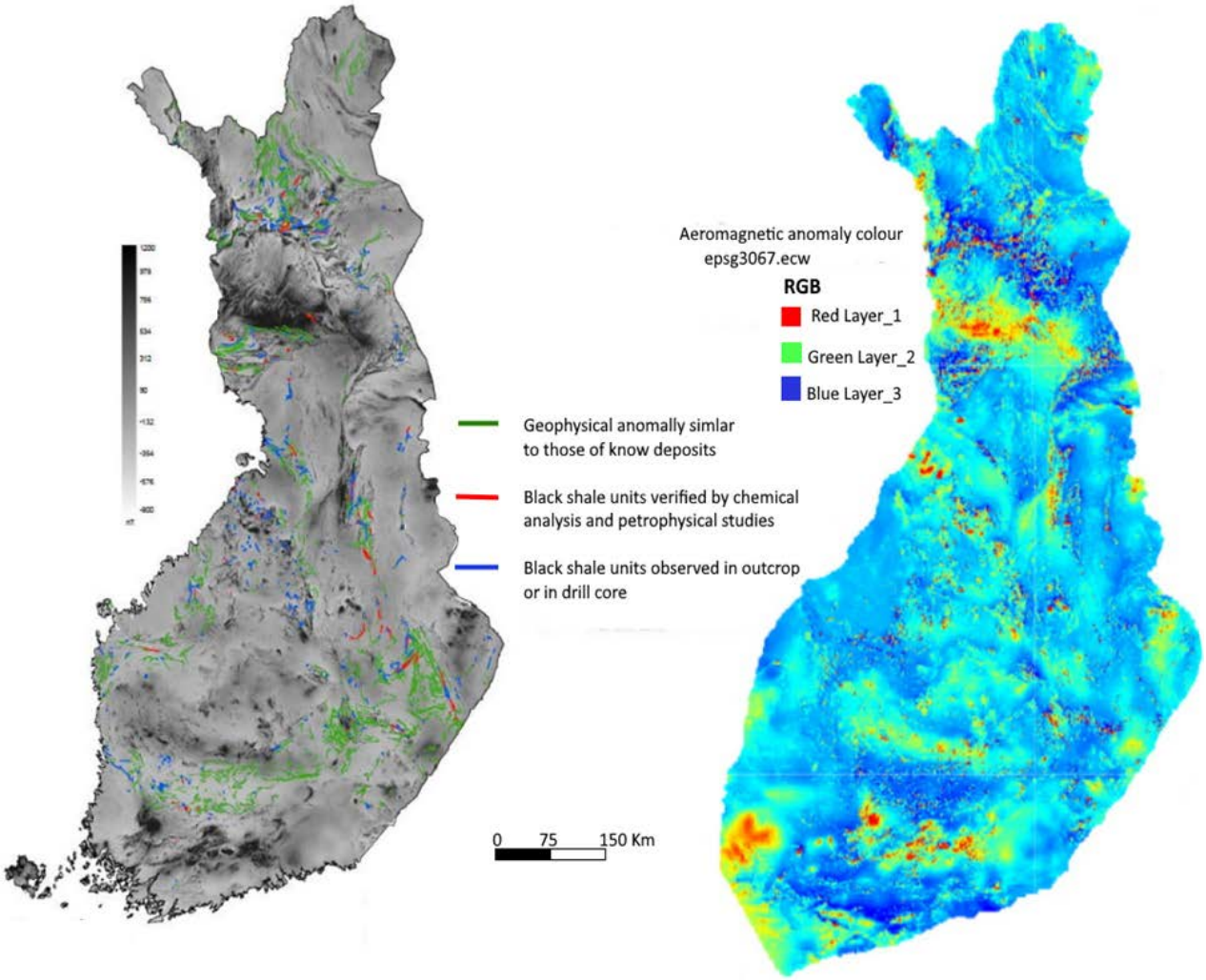

Fig. 3. Aeromagnetic map of Finland with the distribution of black shales as an overlayer, updated from Arkimaa et al. (2000).

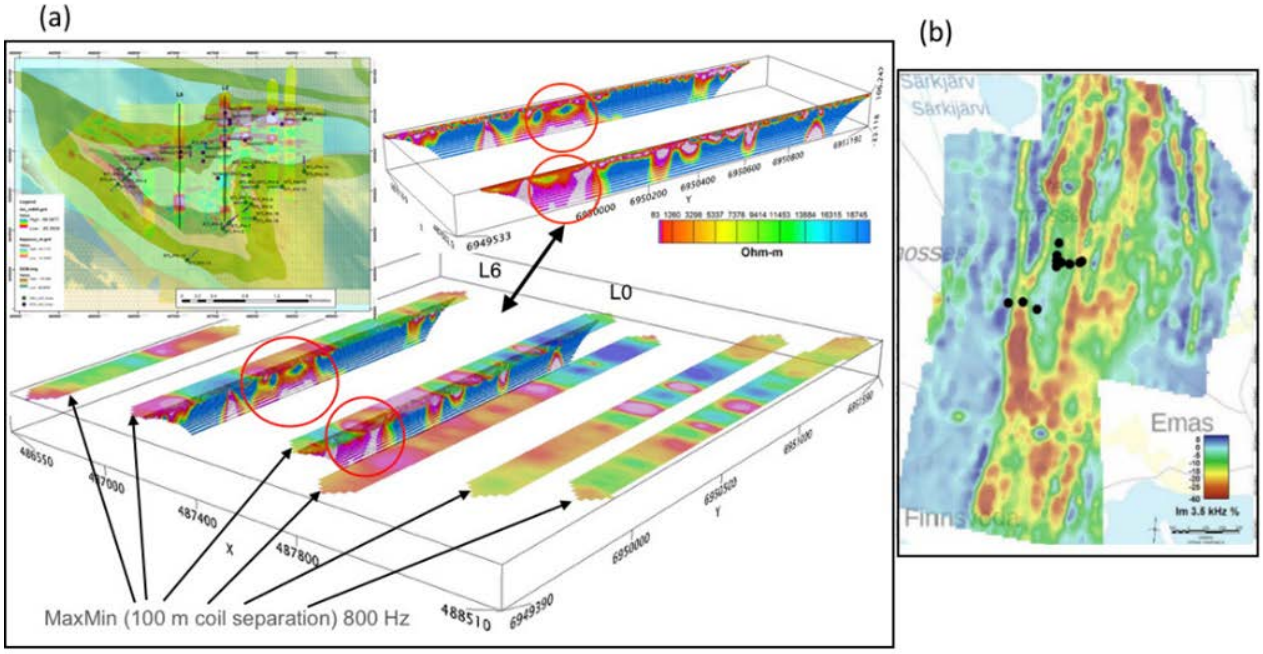

Fig. 4. Geophysical maps of geophysical measurement EM & ERT profiles and drillhole locations at a) Käypysuo and b) Raisjoki graphite occurrences. ERT provided data from a depth of 120 m (L 6 and L 10).

5.2 Core drilling and sampling

The flake graphite-bearing rock samples for this study can be divided into three types: 1) re-logging and re-sampling of an existing drill core in the GTK archive in Loppi combined with new drillholes that were drilled by GTK and Outokumpu Oy, 2) graphite-bearing drill core samples from new drillholes by GTK, and 3) graphite-bearing boulders and outcrops that were collected during fieldwork by GTK geologists. The drill core samples used in this study have been logged and classified with respect to their graphite occurrences. The drill core entirely consists of a finely banded quartz feldspar rock, in which the banding is defined by variation in the content of mica (mostly biotite and chlorite) and of graphite. In parts of the core, the graphite content is low but clearly visible. The graphite appears as good-quality flake graphite with a flakes ranging in size from fine flakes (<150 µm), such as at Raisjoki, to medium flakes (150–400 µm) and coarse flakes (400–1600 µm), found in the Rautalampi–Käypysuo deposit.

5.3 Mineralogical, petrographic, and chemical analysis

Approximately 200 thin sections (30 µm thick) were prepared for the mineralogical and petrographic analysis, cut perpendicular against the foliation and parallel to the stretching lineation whenever possible. This involves the acquisition of digital images of the thin sections and petrographic observations by using a combination of reflected light microscopy for the inspection of opaque minerals and transmitted light microscopy for silicate minerals. Rock specimens were also studied with SEM-EDS, using Hitachi High-Tech's SEM SU3900 with an X-ray detector at the GTK laboratory in Espoo. BSI was used to characterize the mineral morphology and quantity the proportions of primary minerals, while energy dispersive X-ray analysis (EDS) was used for elemental analysis. The goal was to determine the flake size in different graphite-bearing rocks, the characteristics of the graphite flakes and their associated gangue minerals. The SEM and XRD analyses of the graphite revealed that the main impurities are quartz, plagioclase, sulphides (pyrrhotite, pyrite), biotite and chlorite.

The Raman spectra of each sample were recorded using a Renishaw inVia Confocal Raman spectrometer equipped with a Leica DMLM microscope connected to a Leica camera with 5×, 20×, 50×, 100x objectives at GTK Mintec, Outokumpu. Raman spectra were collected on unpolished rock chip surfaces to avoid damage from polishing (e.g., Pasteris 1989, Beyssac et al. 2002). The measurements were performed by using an argon ion laser (785/532) with the extraction wavelength of 532 nm at room temperature with a laser power of 5 mW and a spectrum resolution of approximately 2 cm^{-1}. The spectrum was calibrated against a silicon water standard (520.6 cm^{-1}). Raman measurements of the studied samples revealed a slight shift of all bands (D bands at 1350 cm^{-1}, D2 band at 1620 cm^{-1} and G band at 1580 cm^{-1}). Raman spectroscopy measurements on graphite flakes provide quantitative information on the degree of graphitization, which can be correlated with the grade of metamorphism in the studied areas.

Drill core samples were analysed for major and trace elements by X-ray fluorescence (XRF) and inductively coupled plasma mass spectrometry (ICP-MS) at Eurofins Labtium Oy, Finland. Carbon may be present in the rock in various forms, including organic carbon, carbonates and graphitic carbon. Total C_{gr}, C carbonate and S contents were determined with LECO analysers. The concentration of organic graphitic C_{gr} was calculated as the difference between the total C_{gr} and carbonate C contents.

6 DESCRIPTION OF THE INVESTIGATED FLAKE GRAPHITE OCCURRENCES

6.1 Rautalampi and Käypysuo Graphite exploration

The Käpysuo graphite occurrence in Rautalampi has a high potential for flake graphite due to the quality of the hosted bedrocks and the suitable metamorphic grade. The graphite-bearing rocks have been investigated and determined as satisfying the application requirements to produce high-quality graphite for use as the anode material of lithium-ion batteries (Al-Ani et al. 2018, 2020, 2022).

6.1.1 Graphite Petrology and Mineralogy

More than 1600 m of drill core from 16 boreholes were primarily logged by Timo Ahtola and ~130 thin sections (30 µm thick) were prepared, cut perpendicular against the foliation and parallel to the stretching lineation whenever possible. Käpysuo flake graphite occurs in two rock types: quartz-mica schist and feldspathic biotite gneiss. The quartz-mica schist includes the minerals quartz, feldspar (plagioclase and K-feldspar) and biotite/chlorite as the main minerals. Pyrite and pyrrhotite are dominated by sulphides and associated with graphite and chlorite. The graphite crystals were mostly found to occur along the grain boundaries of other minerals and often arranged in parallel to other minerals, particularly biotite. Graphite flakes plus biotite and chlorite graphite, together with biotite and chlorite, are oriented parallel to the foliation of the rock, a typical texture of the graphite schist (Fig. 5).

Characterization of the size and morphology of graphite flakes is highly relevant in ore evaluation. A representative selection of thin sections was picked for digital microscopy| EM elemental analysis | KEYENCE VHX-7000N image analysis. This involves the acquisition of digital images of the thin sections and the recording of morphological parameters such as the area, perimeter, and longest and shortest axes of graphite flakes. These are automatically recorded for each graphite particle in the examined thin sections. Aggregate measurements from selected thin sections are usually necessary to provide a statistically significant description of the ore. Figure 6 presents an example of such measurements in thin sections N4442018R26_71.35, N4442018R26_109.30, RTL/PH-7_124.00 and RTL/PH-13_175.60, which represented morphological measurements of the graphite aggregate in the Käypysuo area. The dominant size of the graphite flakes is 0.15 mm2 and the mean length of the longest grain axis is 0.30 mm (Fig. 6). Most graphite flakes are 50 to 1600 µm in length, with an oblong shape or platy morphology and a well-ordered crystal lattice, and the ratios between their long and short axes are in the range of 2 to 4 for the flakes. The Käypysuo graphite is characterized by its coarse flakes, which are fully ordered, and its high purity and crystallinity. The results of the graphite morphological data acquisition are important for establishing appropriate procedures for crushing and liberation procedures as a part of the beneficiation tests.

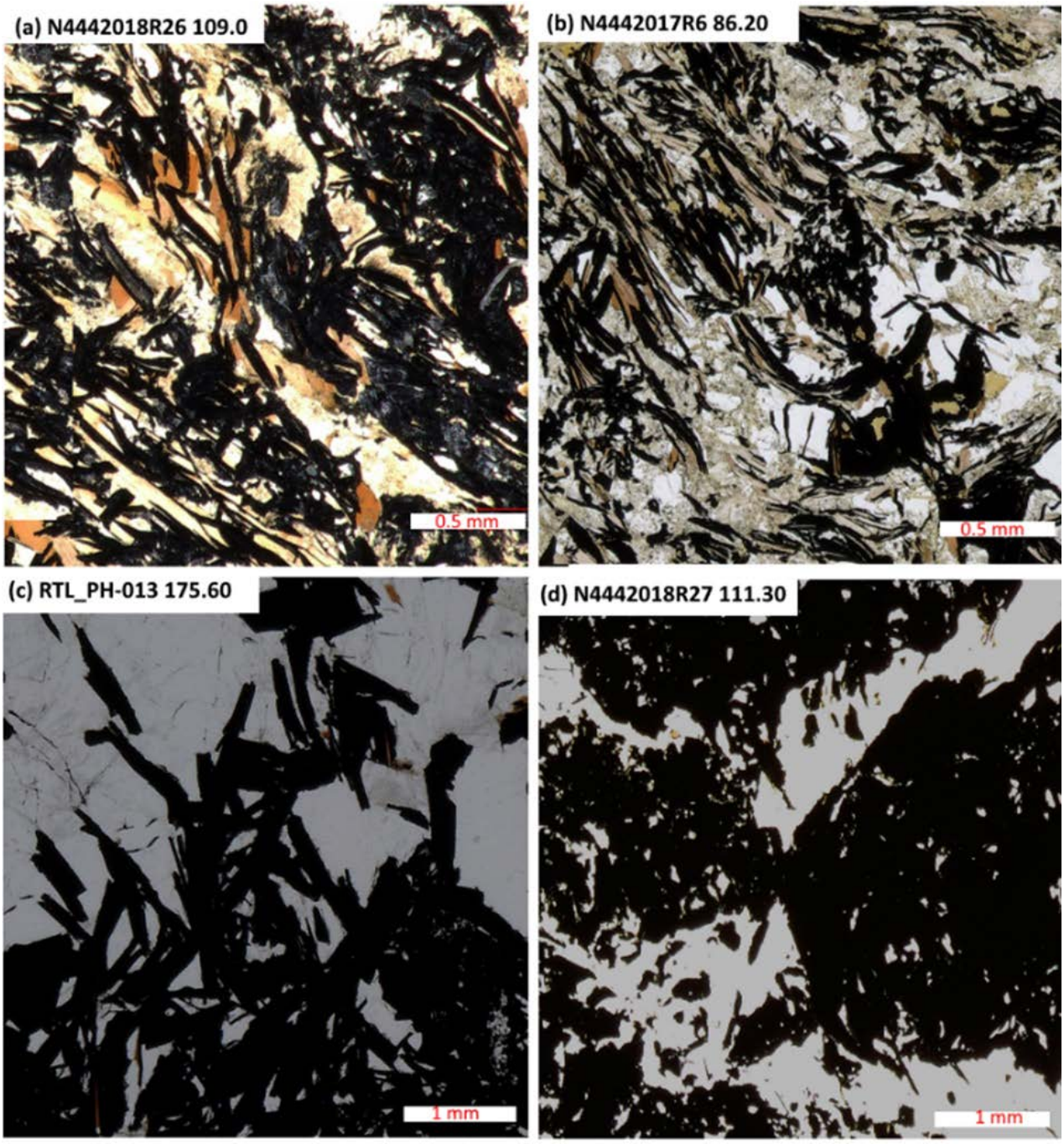

Fig. 5. Petrography of a graphite-bearing schist and gneiss as seen in a polarization microscope, showing large graphite flakes (≥1 mm) occurring as flat, plate-like crystals in the strongly foliated schist consisting of alternating volumes of biotite, quartz, plagioclase, chlorite and sulphide minerals.

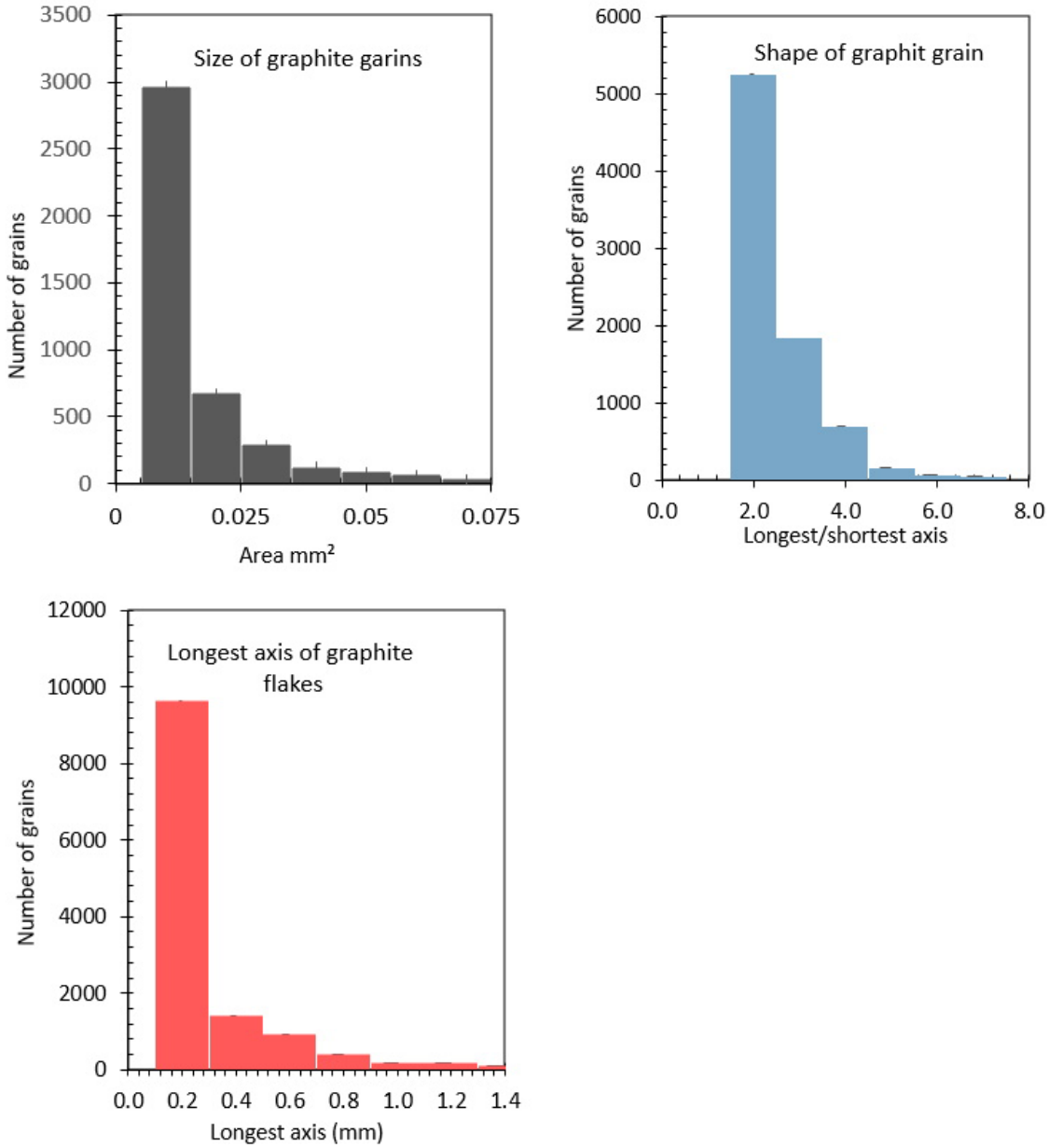

Fig. 6. Histograms showing the morphological variation of the graphite grains in several thin sections. Data were collected by digital microscopy| EM elemental analysis | KEYENCE VHX-7000N image analysis. The data are aggregate measurements of several thin sections and are believed to be representative of the Käypysuo graphite flakes.

We also used scanning electron microscopy (SEM) to assess the size of the graphite flakes in some thin sections of graphite-rich samples. Statistical analysis of three samples (Fig. 7) of the graphite flakes revealed a size (defined as the longest dimension) range from 50 to 1600 µm in length. According to thin section image analysis, most graphite flakes were oblong shaped, but not particularly fibrous, and the ratios between their long and short axes were in the range of 2 to 4 for most flakes. The XRD patterns of ground pure graphite display a strong and narrow peak at 26.6° 2θ and a weaker peak a 54.8° 2θ, which are related to the (002) and (004) reflections of graphite, respectively (Fig. 8a). The lack of any other graphite reflections indicates that the graphite consists of large crystalline flakes oriented in parallel with the sample holder.

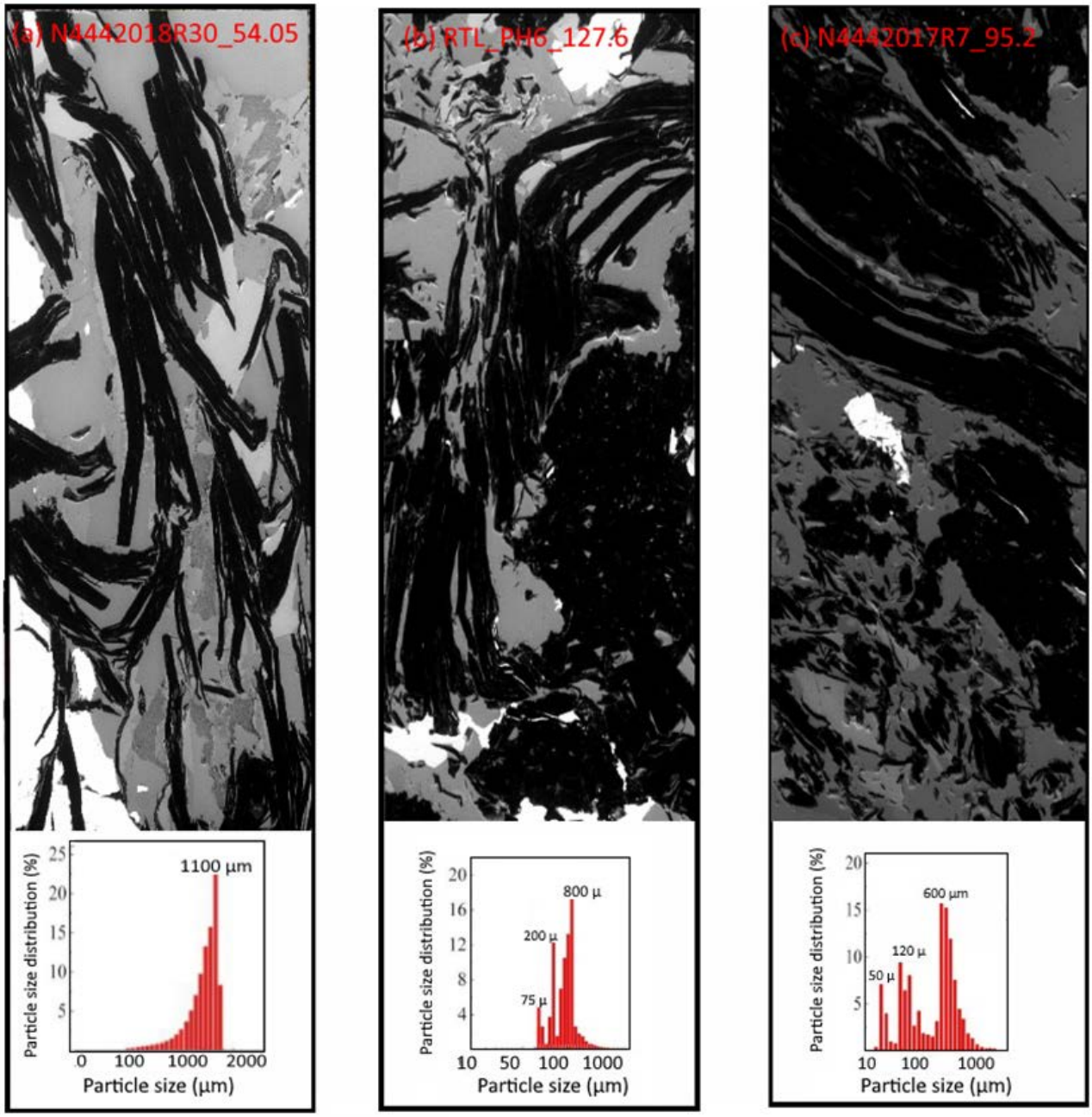

Fig. 7. Graphite flake-size distributions obtained by the analysis of a set of the SEM images of the Käypysuo graphite samples.

6.1.2 Geothermetric modeling

A large variety of experimental geothermometers based on Raman spectra of carbonaceous material (RSCM), bulk compositions and mineral assemblages have been used to estimate the metamorphic temperatures in metasediments and igneous rocks. Three types of geothermometers, namely garnet-biotite (GB), Ti in biotite and RSCM, were used to estimate the metamorphic temperatures for graphite-bearing metapeltic schists/gneisses in Käypysuo, Central Finland.

The GB geothermometer (Holdaway 2000) was applied to three garnet-bearing samples (N4442018R30_90.0, N4442017R7_194.0 and RTL_PH-8_146.9) containing quartz + plagioclase + biotite + garnet with accessory phases of K-feldspar, muscovite, chlorite and graphite. In these selected samples, the garnet porphyroblasts display a homogeneous or weakly zoned core, which is deformed and strongly fractured, filled with chlorite or muscovite, plagioclase and quartz. Temperature–pressure estimates were obtained from garnet porphyroblasts and the adjacent biotite and plagioclase composition with an average of 570 ± 50 °C and 5.6 ± 0.4 kbar for sample N4442018R30_90.0, 635 ± 5 °C and 7.9 ± 0.7 kbar for sample N4442017R7_194.0 and 655 ± 40 °C and 7.8 ± 0.8 kbar for sample RTL_PH-8_146.9 (Fig. 9a,b and Table 2).

The Ti-in-biotite geothermometer provided by Henry et al. (2005) was also used to calculate magmatic biotite temperatures with the following equation:

$$T(°C) = \{[ln\,(Ti) - a - c\,X_{Mg})^3]/b\}^{0.333}$$

where T is temperature in °C, Ti is the apfu normalized to 22 O atoms, X_{Mg} is the Mg/(Mg + Fe) ratio, a = − 2.3594, b = 4.6482×10^{-9} and c = −1.7283.

The estimated temperature based on the Ti-in-biotite geothermometer is consistent with the result inferred from the Ti vs. Mg/(Mg+Fe) diagram (Fig. 9c). The trend for most of the biotite data falls between the temperature contours of ~750 and 700 °C with different values of the X_{Mg} ratio, except for iron-rich biotite data from sample N4442018R30_90.0, which follow the lower temperature contours of ~600 and 500 °C. In low to medium-grade metapelites, biotite rims next to chlorite can be enriched in Fe, possibly due to incipient chloritization of biotite without developing rutile (Henry 1981, Zen 1981). In contrast, distinct local depletion of Ti in biotite near garnet replaced by biotite is also common in high-grade metapelites (García-Casco et al. 2001).

The Raman SCM geothermometer is a promising way to obtain the peak temperature and degree of graphitization. The Raman spectrum of CM is composed of first-order (1100–1800 cm^{-1}) and second-order (2500–3350 cm^{-1}) regions, and the focus of this study was on the former (Fig. 8b). In the first-order region, discriminative bands of the Raman spectrum of CM appear at 1350 cm^{-1} (D1-band), 1580 cm^{-1} (G-band) and 1620 cm^{-1} (D2-band). The relative intensity ratio of D and G bands, R1 = (I_D/I_G), can be used as an indicator of the degree of graphite crystallinity. In addition, the peak metamorphic temperature was estimated using the area ratio (R2), which is defined as R2 = D1/(G + D1 + D2). The ranges of intensity ratios (R1) and peak area ratios (R2) were recorded for the graphite flakes and ranged from 0.002 to 0.20 (mean 0.1 ± 0.04) for R1 and 0.015 to 0.26 (mean 0.11 ± 0.05) for R2.

Several previous studies have demonstrated that the peak metamorphic temperature (T) of regional metamorphic rocks can be estimated by an area ratio (R2) of peaks recognized in Raman spectra of CM (e.g., Beyssac et al. 2002, Aoya et al. 2010). In this study, we adopted the Raman SCM geothermometer calibration by Rahl et al. (2005), which combines both R1 and R2 parameters, with better estimates for a broader temperature range of <350–737 °C.

$$T\,(°C) = 737.3 + 320.9 * R1 - 1067 * R2 - 80.638 * R1^2 \quad (\pm 50\,°C)$$ (Rahl et al. 2005)

The mean values of metamorphic temperatures estimated using the Raman thermometer were 660 ± 50 °C for sample RTL-PH-8_146.9, while the lowest temperature was 550 ± 25 °C for the sample M4121_61_R1_11.8, with a mean value of 620 ± 50 °C. The metamorphic temperatures of other samples, N4442017R7_194.0, N4442018R30_90.0, N4442017R27_102,3 and N4442018R28_162.3, were estimated as 650 ± 45 °C, 620 ± 50 °C, 670 ± 50 °C and 560 ± 30 °C, respectively (Table 5). Figure 9d illustrates that the R1 intensity ratios and area ratios R2 display trends that decrease with increasing metamorphic temperatures, which show that highly crystalline graphite is significantly corre-

lated with metamorphic temperatures with these ratio values. The values of R1 and R2 become smaller with increasing graphite crystallinity and the degree of graphitization.

Our results demonstrate that the metamorphic temperatures estimated with the Ti-in-biotite geothermometer are slightly higher than the metamorphic temperature obtained with the Raman spectroscopy of CM geothermometer, the GB geothermometer, and the conditions obtained from the P–T pseudosections (Al-Ani et al. 2022). However, the mean temperatures estimated in all representative samples display quite similar trends (Table 2). A narrow difference was recorded between the Ti-in-biotite and the other two geothermometers. The temperatures estimated using Ti in biotite are slightly higher than with the GB and Raman geothermometers, being in the range of 0–80 °C.

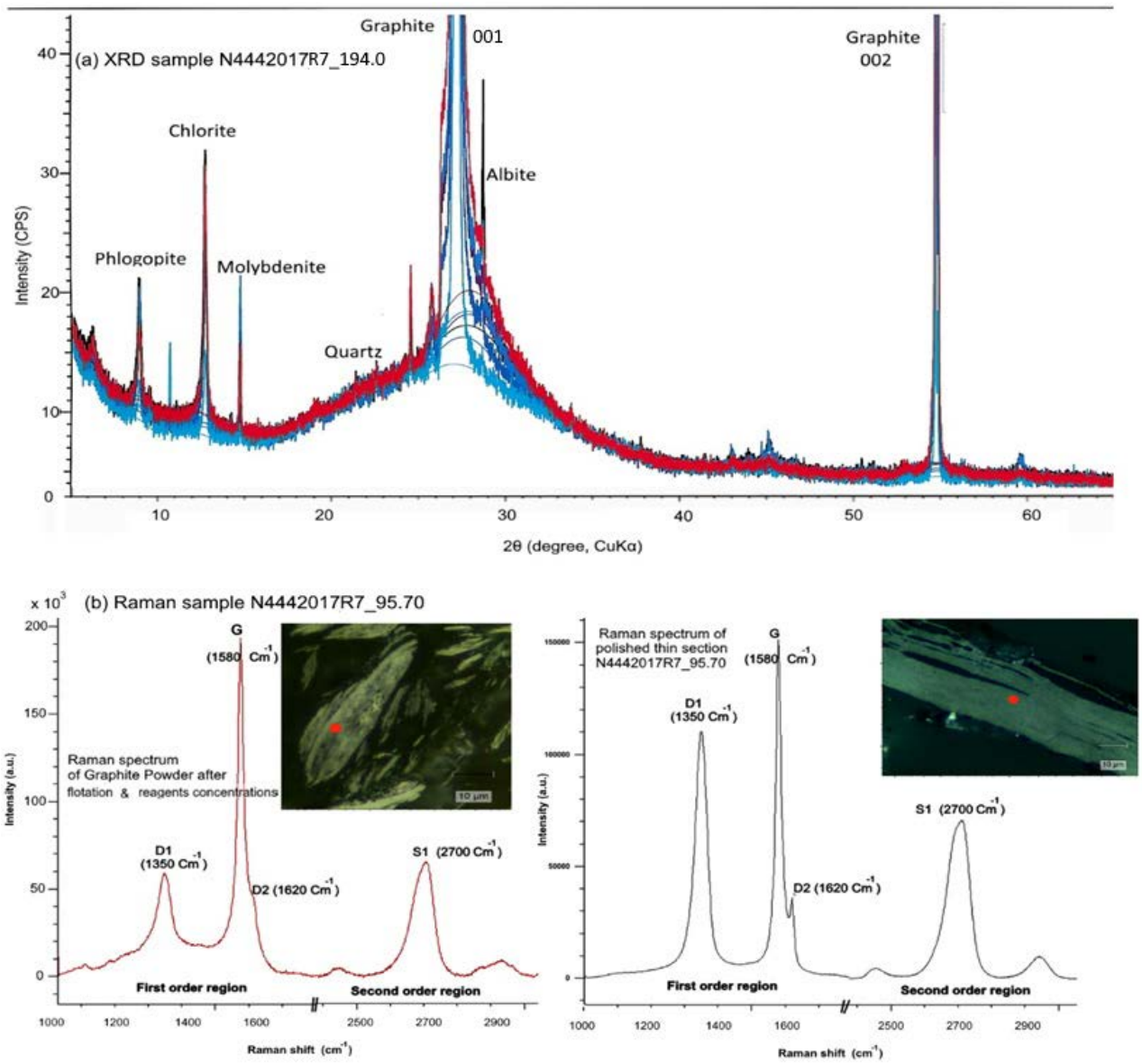

Fig. 8. a) X-ray powder diffraction (XRD) pattern of the sample N4442017R7_194.0. b) Raman spectrum of graphite flakes from sample N4442017R7_95.70.

Table 2. The temperatures (°C) estimated from respective geothermometers in the examined samples.

Sample	GB geothermometer	Ti-Biotite geothermometer	Raman geothermometer	P-T pseudosection
N4442018R30_ 90.0	570±40	570±40	620±50	650-700
N4442017R7_194.0	635±05	710±10	650±45	500-650
RTL_PH-8_146.90	655±05	740±10	660±50	500-650
M4121_61_R1_11.80	No	690±20	550±25	
N4442017R27_102.3	No	730±30	670±50	
N4442018R28_162.3	No	720±50	560±30	

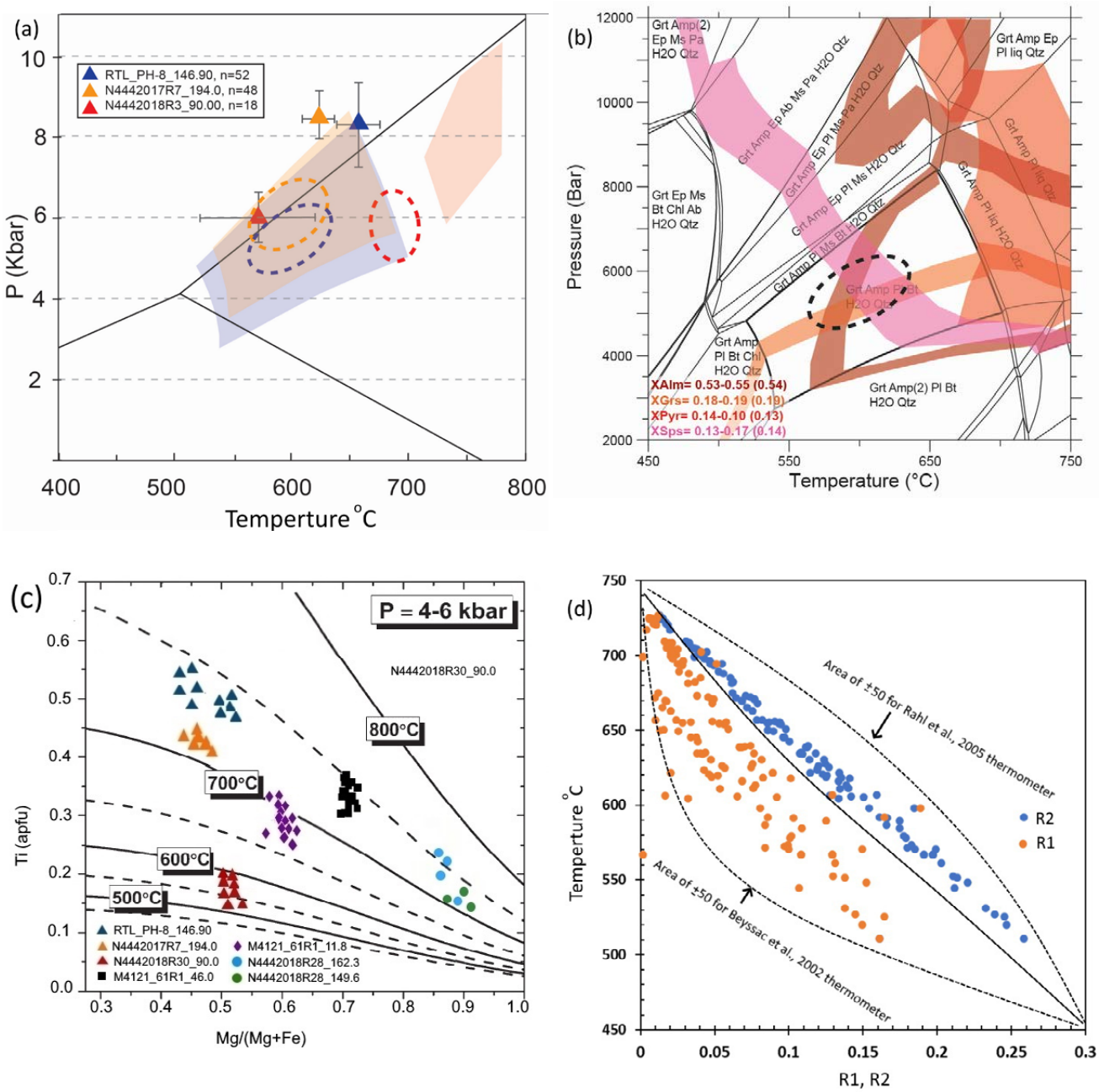

Fig. 9. Respective geothermometers in the examined graphite-bearing samples from Käypysuo. a, b) Calculated T–M and P–T pseudosections for the garnet-bearing samples. c) Ti vs. Mg/(Mg + Fe) diagram (after Henry et al. 2005). d) Relation between (R1, R2) parameters versus independently estimated temperature.

6.1.3 Geochemistry

To calculate the major and trace elemental abundances in Käypysuo graphite occurrences, a total of 554 graphite-bearing rock samples from 34 drill holes were analysed by using a combination of X-ray fluorescence spectrometry (XRF) and inductively coupled plasma mass spectrometry (ICP-MS). The noncarbonate carbon was analysed using the pyrolysis method (ELTRA analyser). The abundances of major oxides (including C_{gr} and S) are listed in Table 3, and statistical histograms of major oxides are presented in Figure 10.

The results highlight the principal oxide available, with a peak composition of 52.44 wt% SiO_2, 13.2 wt% Al_2O_3, 7.6 wt% Fe_2O_3, 2.8 wt% MgO, 2.6 wt% CaO, 2.1 wt% Na_2O, 2.0 wt% K_2O, 2.5 wt% S and 7.0 wt% C_{gr}. The low coefficient of variation (<0.4) and negative skewness of Al_2O_3, SiO_2, Na_2O and K_2O suggest an almost normal distribution, while Fe_2O_3, CaO and MgO, S and C_{gr} show a higher coefficient of variation and positive skewness, which frequently appear towards higher concentrations of sulphides and graphite in some of the studied rocks.

To derive more meaningful graphite abundances, the graphite-bearing rock samples were classified into two types, namely low-graphite and high-graphite samples, based on the C_{gr} content threshold of 10 wt% used in this study. Among the 554 graphite-bearing rock samples, 202 (~50% of the analysed samples) were recorded as having high graphite contents. According to the box-and-whisker plots, the major constituents were SiO_2, Al_2O_3, Fe_2O_3, MgO, CaO, K_2O and Na_2O, in addition to sulphide and graphite (Fig. 11a). The major constituents were commonly related to silicate gangue minerals, i.e., quartz, plagioclase, K-feldspar, biotite with subordinate pyrite, carbonate and chlorite.

Figure 11b illustrates the mineralogical composition of the graphite-rich samples (>10 wt%) in a box-and whisker plot. The mineral proportions of the whole rock major element were calculated using the MINSQ program (Herrmann & Berry 2002). Box-and-whisker plots in general show a low symmetry distribution of the data. From a simple observation of the graphic, it is extremely easy to compare the mineral composition of the samples, considering the medians values as well as the dispersion of the data and the outliers. In this sense, the most significant differences could be observed in the major constituents: quartz, plagioclase and graphite contents are distinctly higher than those of the other minerals. The range in the respective mineral values is also distinctly higher than in the other classes, such as mainly quartz (11.2–46.57 wt%), plagioclase (2.5–31.0 wt%), graphite (10.0–38.0 wt%) and biotite (0.15–36.5 wt%), followed by chlorite, muscovite, pyrite, calcite, K-feldspar, and so on. The highest content of graphite is remarkable in drill hole RTL_PH-007 and in the depth ranges 138.10–138.85 and 158.10–158.85 RTL_PH-007 138.10–138.85.

Table 3. Statistical properties of major elements and graphite (wt%) in 554 samples collected from 34 drill holes in Käypysuo graphite occurrences.

Oxide	Al_2O_3	Fe_2O_3	MgO	SiO_2	CaO	Na_2O	K_2O	S	C_{gr}
Min	5.56	2.16	0.97	15.36	0.30	0.21	0.24	0.09	5.20
Max	20.68	48.81	12.30	71.85	20.31	4.49	5.20	19.26	38.0
Mean	13.25	7.63	2.80	52.44	2.57	2.05	1.98	2.54	12.01
Stdv.	2.32	4.57	1.29	9.15	1.99	0.79	0.76	2.04	6.41
Coefficient of Variation	0.17	0.60	0.46	0.17	0.77	0.39	0.38	0.81	0.91
Skewness	-0.05	4.52	2.04	-0.28	2.76	-0.09	0.49	3.55	1.23

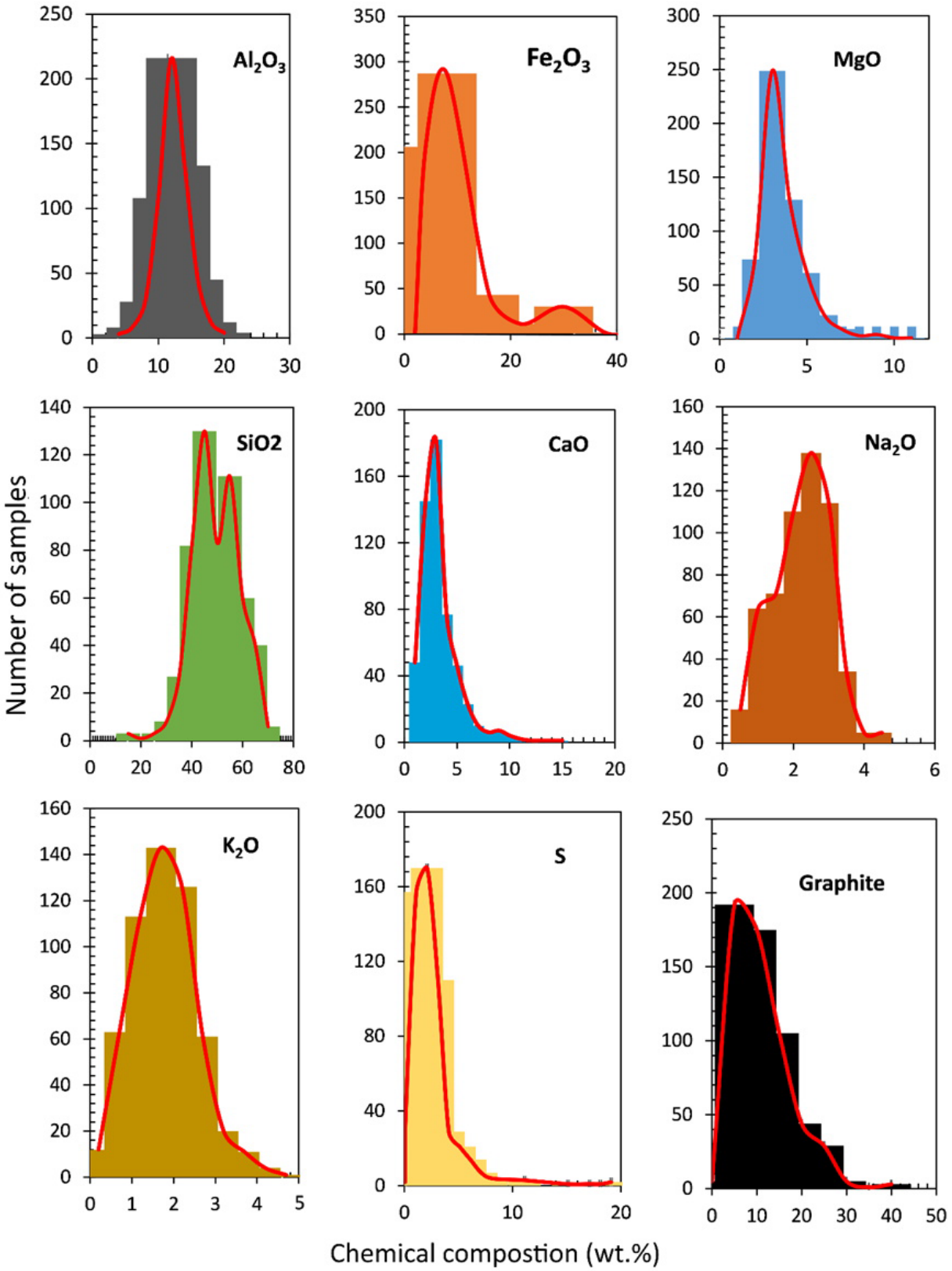

Fig. 10. Histograms of major oxide and graphite wt% values from the 554 samples analysed from the Käypysuo graphite occurrence, Central Finland. The red curve in each chart is an overlain normal distribution curve.

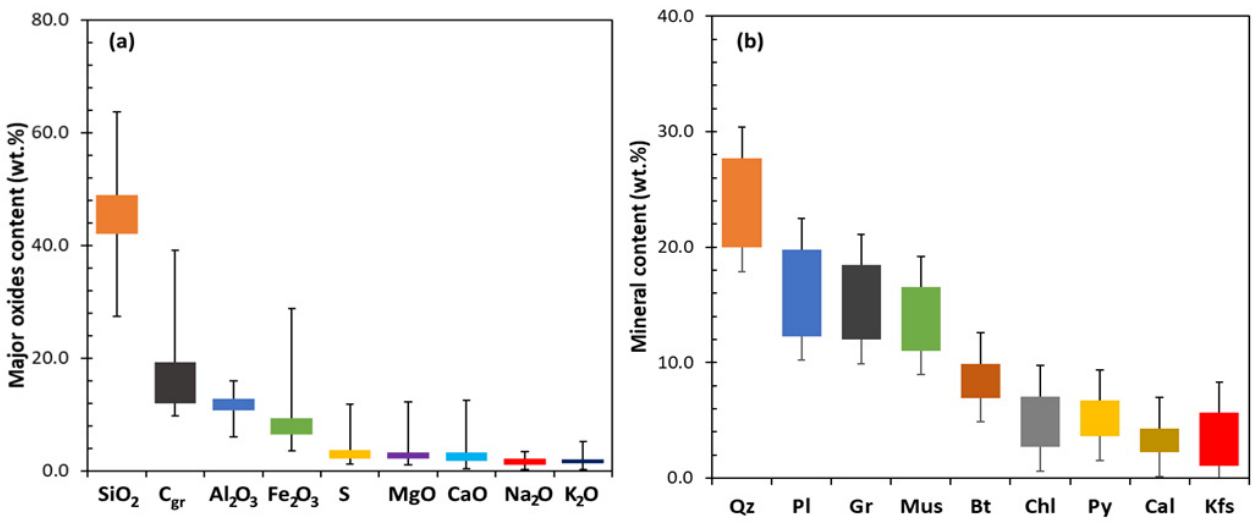

Fig. 11. Chemical composition of the graphite-rich samples in Käypysuo. a) Box-and-whisker plot for the major oxides. b) Mineralogical phases in the graphite-rich samples (>10 wt%). (Qz = quartz, Pl = plagioclase, Gr = graphite, Mus = muscovite, Bt = biotite, Chl = chlorite, Py = pyrite, Cal = calcite, Kfs = potassium feldspar).

6.2 Raisjoki Graphite exploration

The Raisjoki area is located entirely within the easternmost part of the Paleoproterozoic Svecofennian schist belt, bounded to the west by the Vaasa complex (VC) and to the east by the Hallapuro formation (Ha) mafic volcanic rocks and the Central Finland Granitoid Complex (CFGC) (Fig. 12). The Raisjoki area includes several explorations targets: Raisjoki (Ni–Co, graphite), Emas (graphite, Ni–Co–Au), Kaitåsen (graphite, Ni–Co) and Honka (Li–Ni–Co). These targets also belong to N–S-trending mafic to ultramafic volcanic sequences associated with metasedimentary metavolcanic rocks, which host several notable features, including graphite and Ni–Co–Zn mineralization. Here, we focus on the mineralogical characterization of graphite in Raisjoki–Emas, and we also describe the flotation separation and purification techniques to produce high-quality graphite. A total of 20 graphite-rich samples for mineralogical analysis and 87 samples for whole-rock analyses were collected from 4 drill holes in the Raisjoki target and 4 drill holes in the Emas target (Fig. 12 and Table 4). The mineralogical characterization and textural relations of the minerals were carried out on both graphite-bearing rock samples and final graphite concentrates.

Table 4. Drilled boreholes data in Raisjoki targets.

Targets/Borehole	Borehole depth (m)	Location		Analysis	
		x-coordinate	y-coordinate	Thin sections	Chemistry
P4222019R3	127	331145.88	7035101.54	5	21
P4222019R4	97	331092.77	7035048.65	3	23
P4222019R5	96	331174.47	7034934.65	1	10
P4222019R6	114	330946.06	7035186.62	1	12
P4222019R20	113	325881.77	7045028.99	2	4
P4222019R21	129	325883.48	7045059.59	2	5
P4222019R22	115	325880.57	7044996.28	3	5
P4222019R24	130	325895.57	7045130.11	2	4
P4222019R25	96	325959.42	7045010.90	1	3
Total	1017			20	87

6.2.1 Graphite Petrology and Mineralogy

Graphite mineralisations in the Raisjoki area are hosted by sulphur-graphite black schists and amphibolite, and less commonly by metavolcanic interlayers. The number of graphite-rich zones and their strike lengths were estimated using the available geophysical and geological information from each locality. The thicknesses of the units were estimated from geophysical data and drilling. A 3D geological model of the Raisjoki area indicates that graphite-rich black schist layers extend for tens of kilometres towards the NW–SE, with thicknesses ranging from a few metres up to 40 metres (Kuusela et al. 2022).

The graphite schists show strongly foliated fabric due to the compositional layering and preferred orientation of the mica (biotite, phlogopite) and graphite–sulphide minerals (Fig. 13a,b). Graphite and sulphide are the main opaque minerals. Major sulphide minerals observed in the Raisjoki area are pyrrhotite and hexagonal pyrite. Sphalerite and chalcopyrite occur in trace quantities. Sulphide minerals occur as dissemination in intergranular spaces between silicate matrixes, as polycrystal aggregates in quartz-veins and quartz clusters, and within shear zones that have both biotite and graphite (Fig. 13c,d).

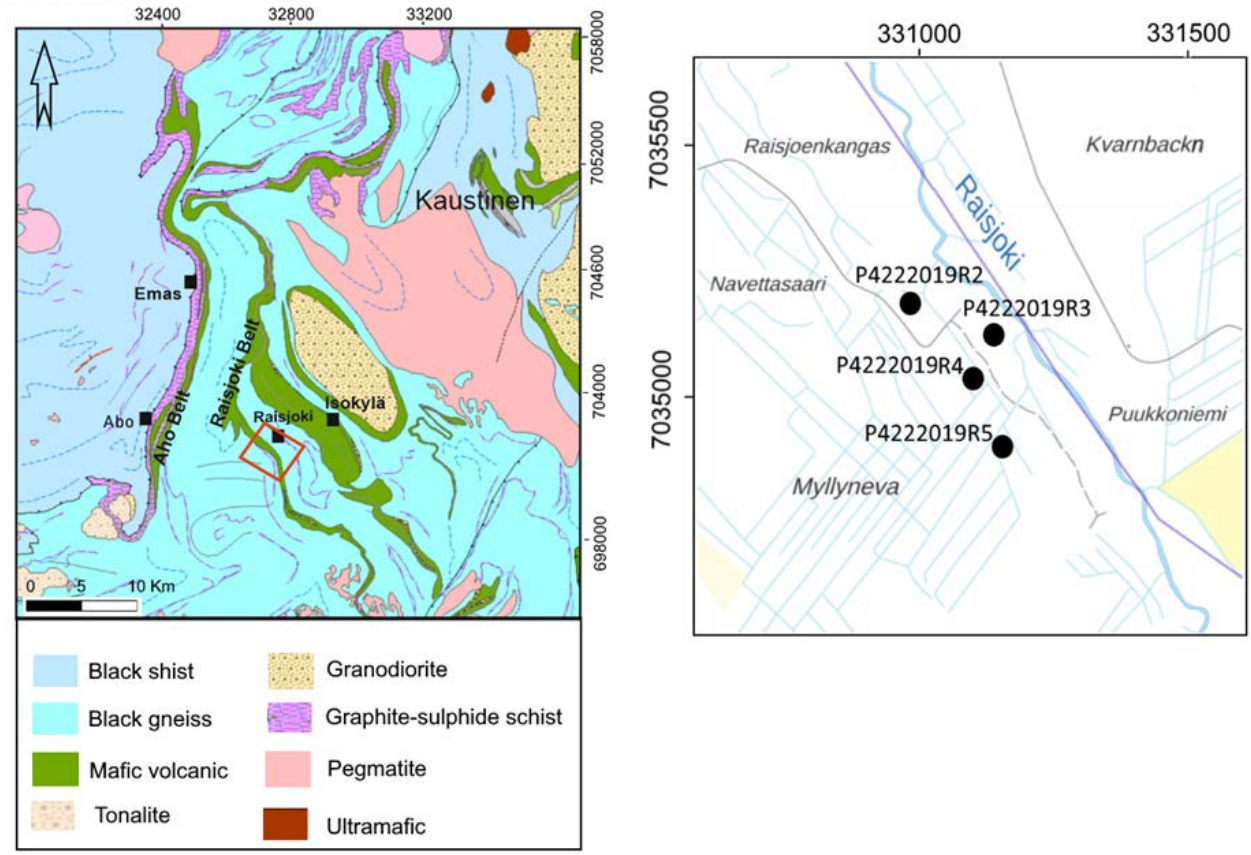

Fig. 12. Geological map of the Raisjoki–Emas area and enlarged map of the study area showing borehole locations. (Bedrock of Finland – DigiKP). Base map © National Land Survey of Finland.

Graphite flake sizes range from 30 to 100 µm, with the majority being 50 µm in length and in some cases even finer. In addition, a few graphite crystals occur very irregularly distributed in the rock, and there is large variation in both the grain size distribution and the area percentage of graphite within a small area, even at the thin section scale.

Various thin sections from Raisjoki were selected for microscopic image analysis using an EM KEYENCE VHX-7000N Digital Microscope. This involves the acquisition of digital images of the thin sections, and after multi-step processing, morpho-

logical parameters such as the area, perimeter, and the longest and shortest axes of graphite grains are recorded. The dominant size of the graphite flakes is 0.01 mm2 and the mean length of the longest grain axis is 0.02 mm. Most graphite flakes are oblong shaped, but not particularly fibrous, and the ratios between their long and short axes are in the range of 1 to 3 for most of the flakes (Fig. 14).

The graphite flake size distributions calculated from SEM images are also presented in Figure 15. According to the SEM images and histograms, the size of individual graphite crystals in the studied rock samples varies from 30 to 150 µm, with flakes often having a mean length of 50 µm and in some cases even finer.

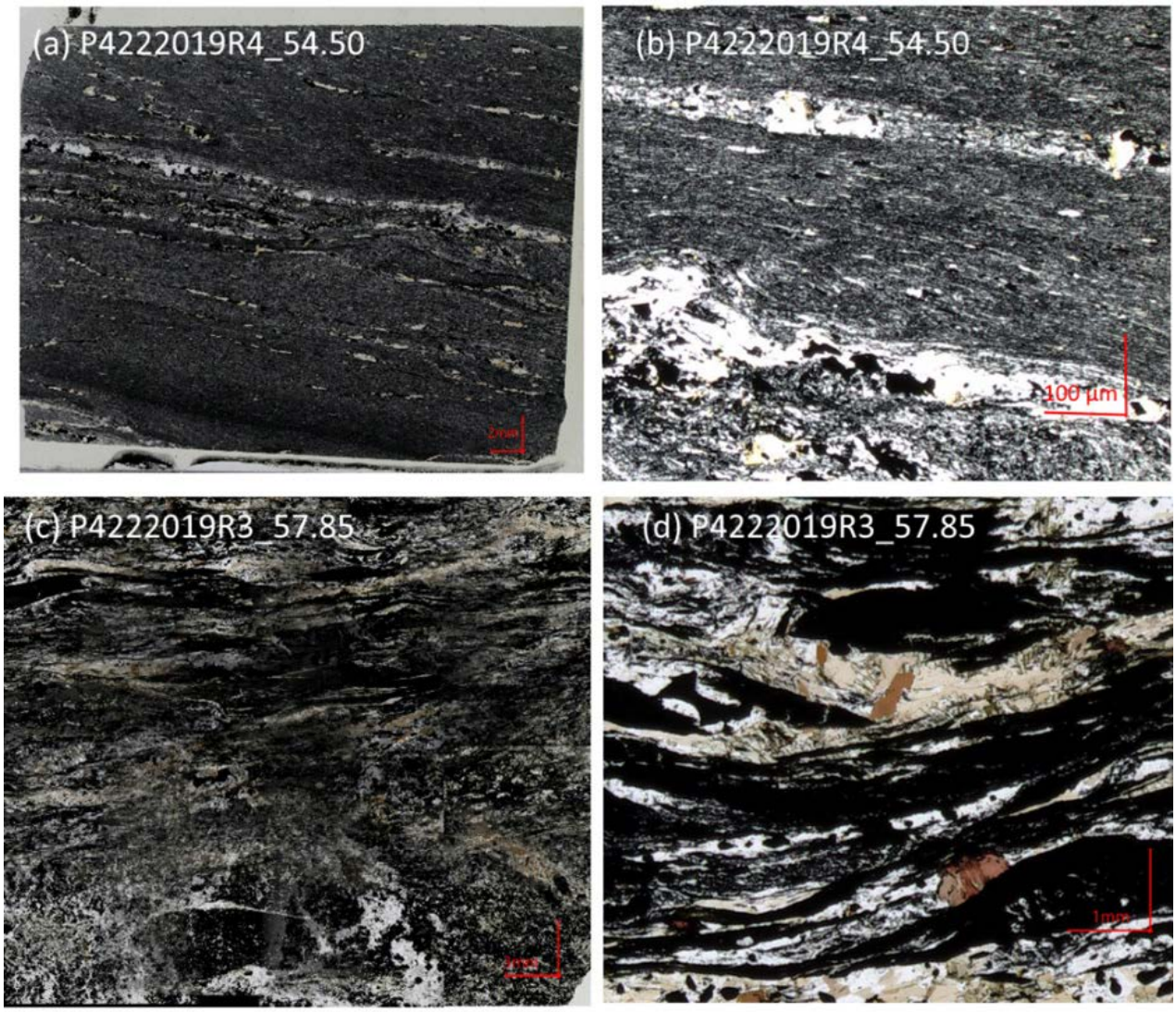

Fig. 13. Thin sections of graphite-bearing rocks showing a preferred orientation parallel to foliation and schistosity of the studied black schist rocks and the size and amount of graphite flakes often with mean length of 50 µm and some cases even finer. (Thin sections P4222019R4/54.50 and P4222019R3/57.85, with graphite and sulphide contents of 8.1 C% and 10.5 S% and 9.2 C% and 5.6 S%, respectively).

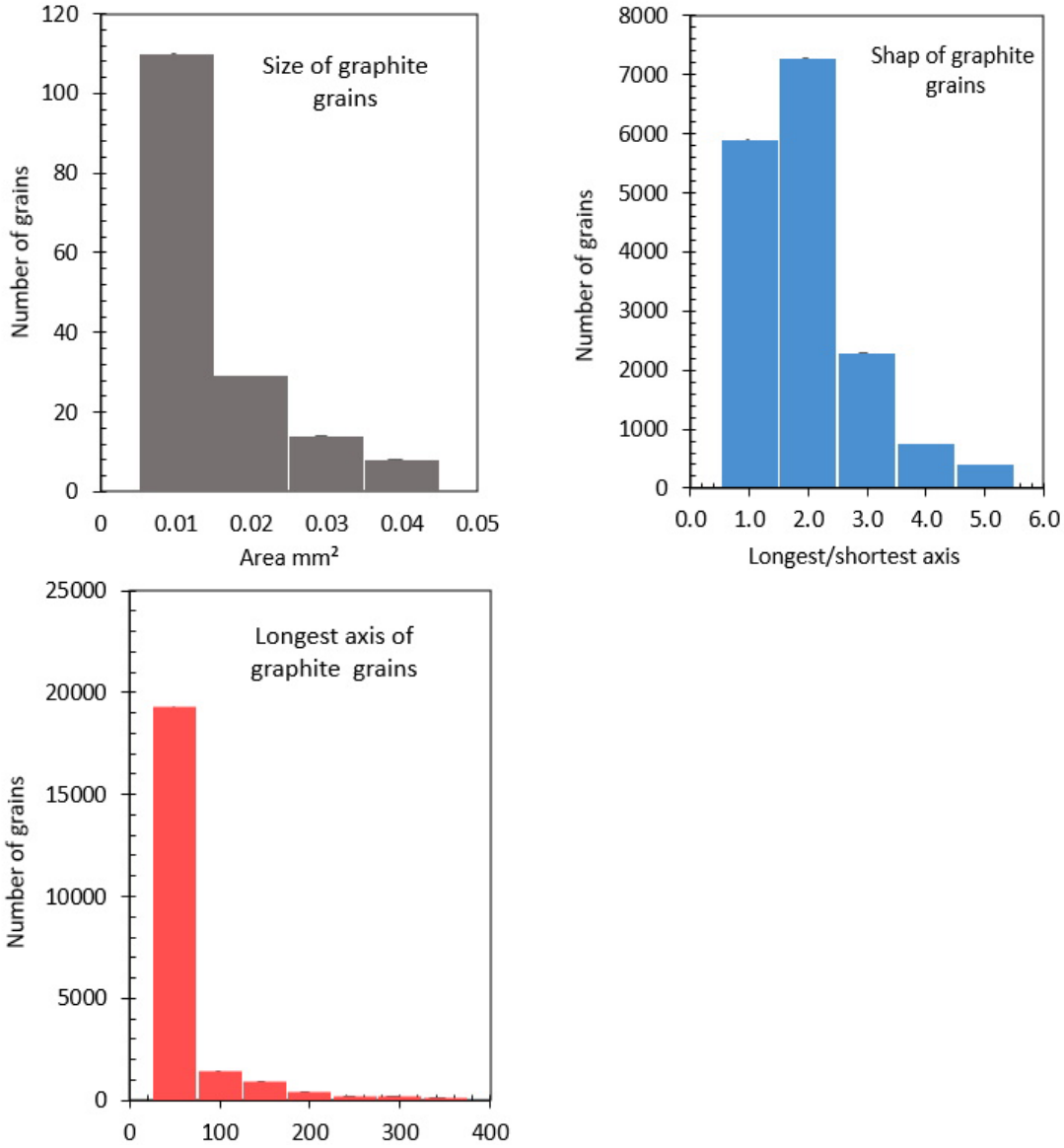

Fig. 14. Histograms showing the morphological variation of the graphite grains in various thin sections. Data were collected by digital microscopy| EM elemental analysis | KEYENCE VHX-7000N image analysis. The data are aggregate measurements of many thin sections and are believed to be representative of Raisjoki graphite grains.

The calculated graphite flake size distributions by SEM images are also presented in (Fig. 15). The SEM images and histograms show crystals size of individual graphite crystals in the studied samples rock varies from 30 to 150 µm with flakes often in mean length of 50 µm and in some cases even finer.

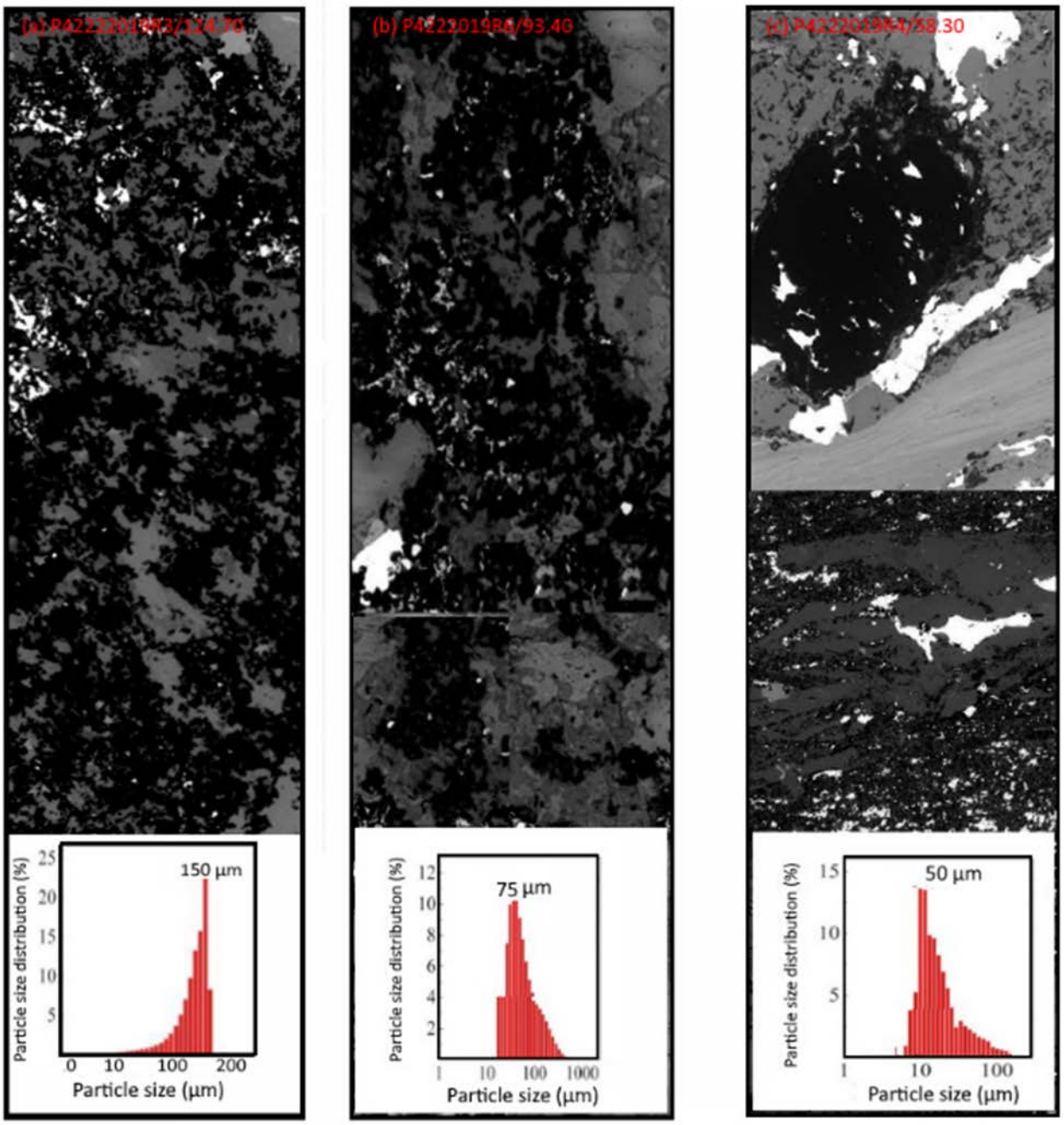

Fig. 15. Graphite flakes size distributions obtained by the analysis of a set of the SEM images of the Raisjoki graphite samples.

6.2.2 Raman geothermometer

A major application of Raman spectroscopy in the study of CM is to derive peak metamorphic temperatures from spectra collected on graphite-rich samples. The CM geothermometer utilizes a combination of R1 and R2 parameters, defined as the intensity ratio, R1 = (I_D/I_G), and the peak area ratio, R2 = D1/(G + D1 + D2).

A wide range of intensity ratios (R1 and R2) were recorded for the graphite particles in 10 thin sections selected from Raisjoki graphite (Fig. 16a,b), ranging from 0.91 to 0.34 for R1 and 0.37 to 0.48 for R2 (Fig. 16c), indicating that the graphite formed in medium-grade metamorphic terrains under medium temperatures (496 ± 14 °C to 428 ± 20 °C).

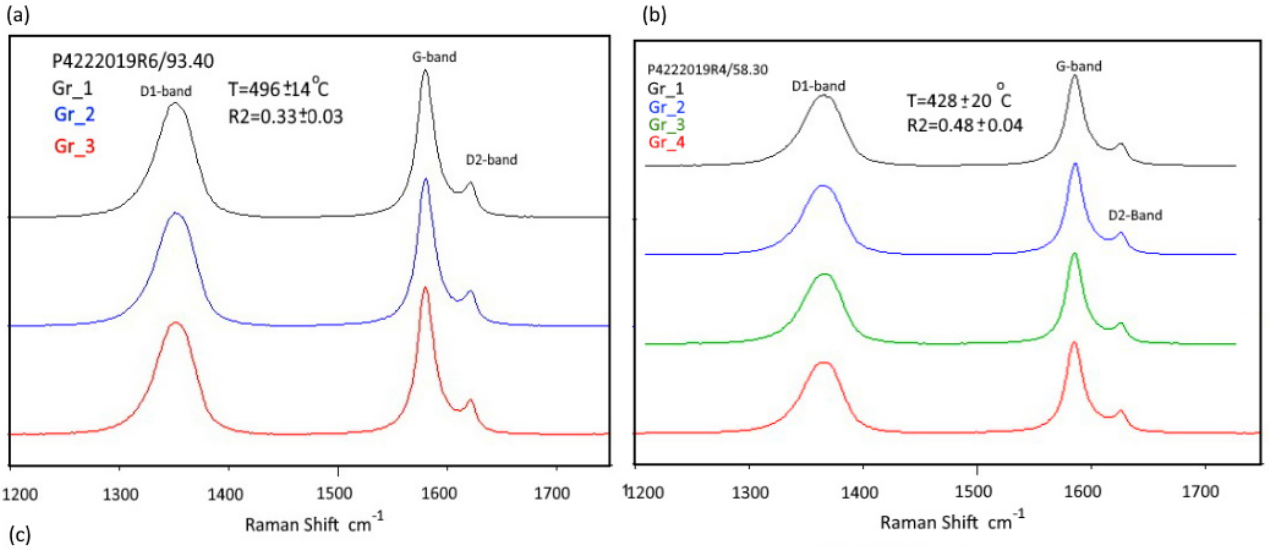

(c)

Spectrum	Peak Position			FWHM			R1	R2	TGr (°C)*	TGr (°C)**
Sample	D1	G	D2	D1	G	D2				
P4222019R3/15.10	1351	1581	1622	42	17	7	0.58±0.2	0.37±0.05	478±19	469±21
P4222019R3/15.60	1353	1582	1624	41	17	8	0.83±0.01	0.42±0.02	453±8	443±8
P42222019R3/57.85	1351	1581	1622	42	17	7	0.82±0.09	0.42±0.05	454±24	444±24
P42222019R3/124.70	1350	1579	1622	42	18	7	0.70±0.1	0.39±0.03	468±14	458±14
P4222019R4/54.50	1351	1580	1627	44	20	7	0.58±0.2	0.40±0.01	465±8	454±8
P4222019R4/58.30	1348	1580	1621	40	18	7	0.91±0.1	0.48±0.04	428±20	418±18
P4222019R4/61.60	1350	1580	1622	41	17	7	0.65±0.2	0.38±0.1	471±8	461±9
P4222019R6/93.40	1344	1571		51	32		0.34±0.1	0.33±0.03	496±14	488±16

* Beyssac et al., (2002)
** Aoya et al. (2010)

Fig. 16. a, b) Raman spectra parameters obtained from Raisjoki graphite samples. c) R1, R2 values and temperatures for each sample are also indicated.

6.2.3 Geochemistry

More than 60 graphite- and sulphide-bearing rocks samples from Raisjoki target were analysed for major and minor elements by using a combination of ICP-OES and ICP-MS. The non-carbonate carbon was analysed using the pyrolysis method (ELTRA analyser). In the graphite- and sulphide-bearing rocks from the Raisjoki area, the organic C content varies from 5.3 wt% to 11.5 wt% (avg. 8.4 wt% C) and the S content from 2.9 to 18.3 wt% (avg. 6.9 wt% S) (Table 5). Furthermore, the rocks are characterized by low abundances of SiO_2 (25.0–54.2 wt%), and high contents of Fe_2O_3 (7.5–29.2 wt%), MgO (1.7–8.1 wt%), CaO (1.7–10.7 wt%), Al_2O_3 (6.1–15.3 wt%), Na_2O (0.7–3.7 wt%), K_2O (0.6–2.9 wt%), P_2O_5 (0.1–0.3 wt%) and TiO_2 (0.2–1.4 wt%) (Table 5). A box-and-whisker plot of the major chemical constituents in the Raisjoki area generally illustrates a low symmetry distribution of the data. The highest content dispersions are observed for SiO2 and Fe2O3, followed by graphite and sulphides (Fig. 17a).

Through the identification of graphite by using optical microscopy/SEM, organic C is graphite and S occurs in pyrrhotite and pyrite. Normative mineralogy by using the MINSQ program (Herrmann & Berry 2002) is a valuable tool for interpreting the mineralogical composition of rocks based on their bulk rock geochemical data. The gangue minerals are quartz (2.6–28.5%), plagioclase (5.4–45.3 wt%), K-feldspar (0.0–11.9 wt%), biotite (0.1–19.1 wt%), muscovite (0.0–20.6 wt%) and chlorite (5.5–22.2 wt%), followed by calcite and apatite. The ore minerals are graphite (5.4–11.4 wt%) and sulphides (7.0–28.3 wt%), as seen from the mineralogical composition of the graphite-bearing samples in the box-and-whisker plot (Fig. 17b).

Table 5. Statistical properties of major elements and graphite (wt%) in 60 samples collected from 4 drillholes in the Raisjoki–Emas graphite occurrences.

Sample	SiO_2	Al_2O_3	Fe_2O_3	MgO	CaO	Na_2O	K_2O	S	C_{gr}
Min	25.03	6.05	7.49	1.69	1.72	0.67	0.60	2.89	4.14
Max	54.21	15.29	29.17	8.07	10.72	3.73	2.90	18.30	11.50
Stdv.	6.40	1.92	4.62	1.50	1.92	0.67	0.59	3.27	2.29
Avg.	40.55	10.44	18.88	3.59	4.42	2.05	1.57	7.77	6.85
Coefficient of Variation	0.16	0.18	0.24	0.42	0.44	0.33	0.37	0.42	0.33
Skewness	0.03	0.46	-0.32	0.99	0.92	0.32	0.22	1.36	0.50

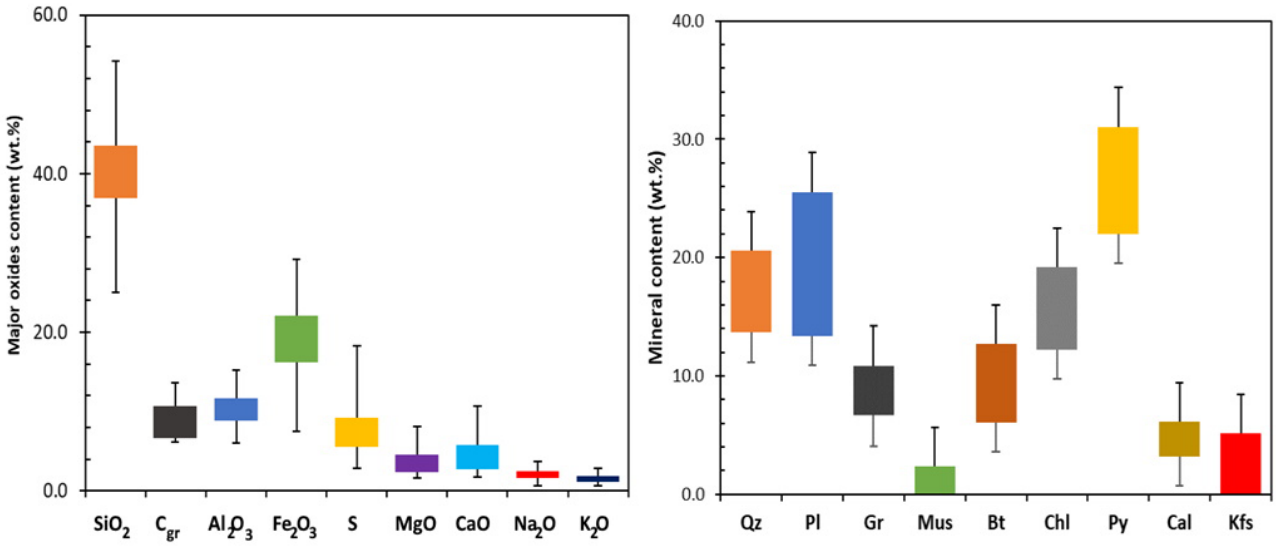

Fig. 17. Chemical composition of the graphite-bearing rocks in Raisjoki a) Box-and-whisker plot for the major oxides, b) mineralogical phases in the graphite-rich samples (> 5 wt.%). (Qz = quartz, Pl = plagioclase, Gr = graphite, Mus = muscovite, Bt = biotite, Chl = chlorite, Py = pyrite, Cal = calcite, Kfs = potassium feldspar).

6.3 Joutsijärvi-Kuusivaara Graphite exploration

The investigated area is situated in the eastern part of the Central Lapland Granitoid Complex, approximately 25 km east of Kemijärvi (Fig. 18). This area has previously been examined by GTK for base metals and gold (Pankka 1999). Magnetic and electromagnetic geophysical surveys were conducted during 1995–1997, revealing electromagnetic anomalies associated with the presence of sulphides and layers rich in flake graphite in the investigated area. GTK drilled twenty-two shallow diamond drill holes (totalling approximately 656 m) and six deep diamond drill holes (totalling approximately 625 m) in 1996.

The mineralogy and geochemistry of the graphite schist from the Joutsijärvi and Kemijärvi areas in Northern Finland were studied. In the investigated area, two types of rocks were found to contain a significant amount of graphite: graphite flakes occurring in strongly foliated graphite–sulphide–schist and disseminated graphite flakes within a banded gneiss. More than 20 drill core samples were analysed using X-ray powder diffractometry to measure the graphitizing degree, in combination with petrographic microscopy, scanning electron microscopy (SEM-EDS) and X-ray fluorescence (XRF) analysis.

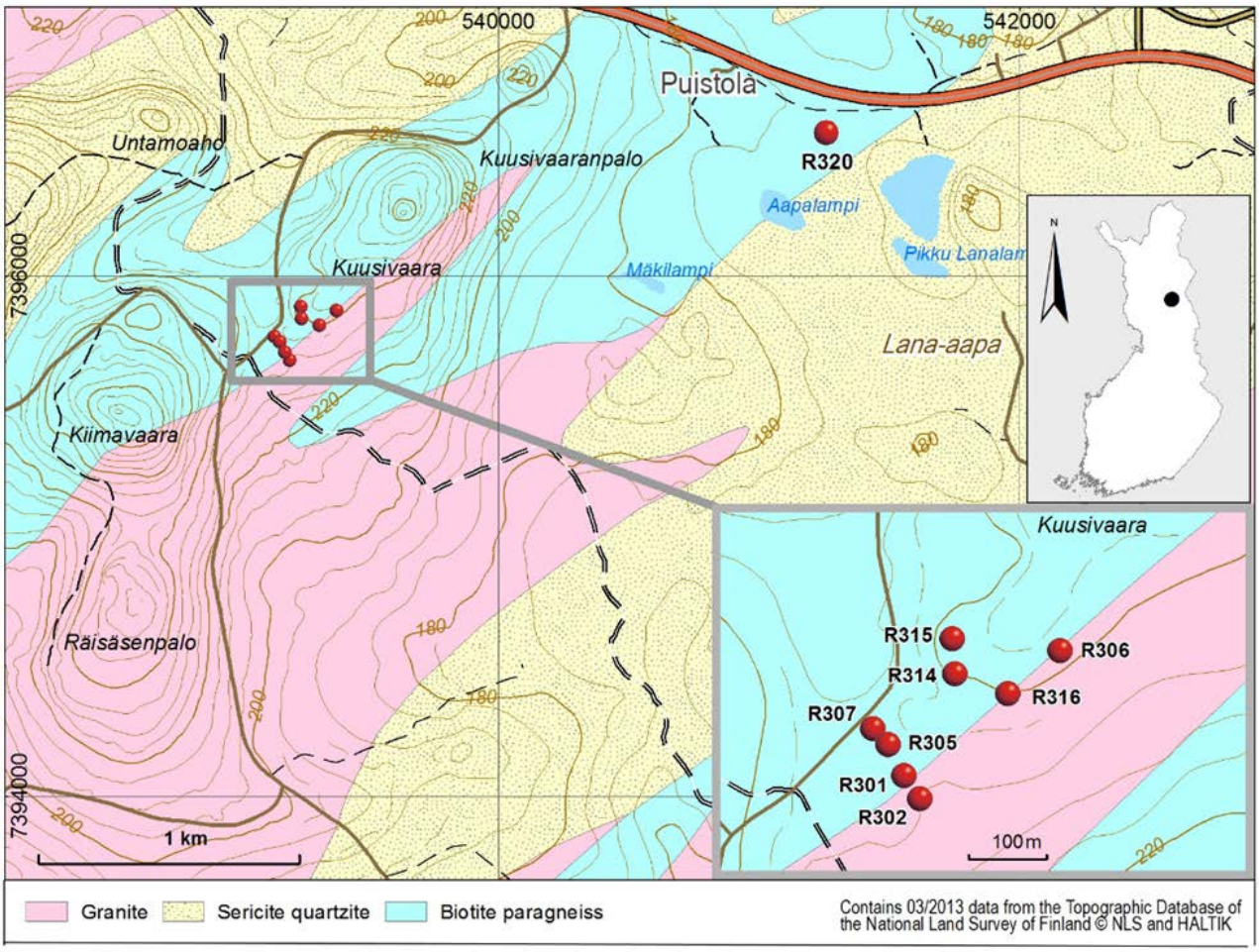

Fig. 18. Geological map of the Joutsijärvi–Kuusivaara area showing borehole locations. [Bedrock of Finland – DigiKP). Base map © National Land Survey of Finland.

6.3.1 Graphite Petrology and Mineralogy

Graphite flakes generally occur in strongly foliated rocks in which the foliation is defined by the parallel orientation of the graphite flakes. The main gangue minerals are quartz, plagioclase and K-feldspar, with subordinate chlorite and biotite (Fig. 19). The graphite flakes were found to range in size from 100 µm 2000 µm and graphite shows good orientation with flakes, frequently with a mean length of 400 µm. Most graphite flakes are oblong shaped, but not particularly fibrous, and the ratios between their long and short axes are in the range of 2 to 4 for most of the flakes. The Kuusivaara graphite is also characteristic of a coarse and high-quality flake graphite, with properties similar to those of Käpysuo graphite. Representative thin sections were selected for digital microscopy examinations, and morphological parameters such as the area, perimeter, and the longest and shortest axes of the graphite flakes were recorded. Most graphite flakes are oblong shaped, the dominant size of the flakes being 0.1 mm2, the mean length of the longest grain axis is 0.15 mm, and the ratios between their long and short axes are in the range of 2 to 4 for most of the flakes (Fig. 20). The graphite grains are situated interstitially between the grain boundaries of gangue silicates, and more rarely as inclusions in the silicate minerals.

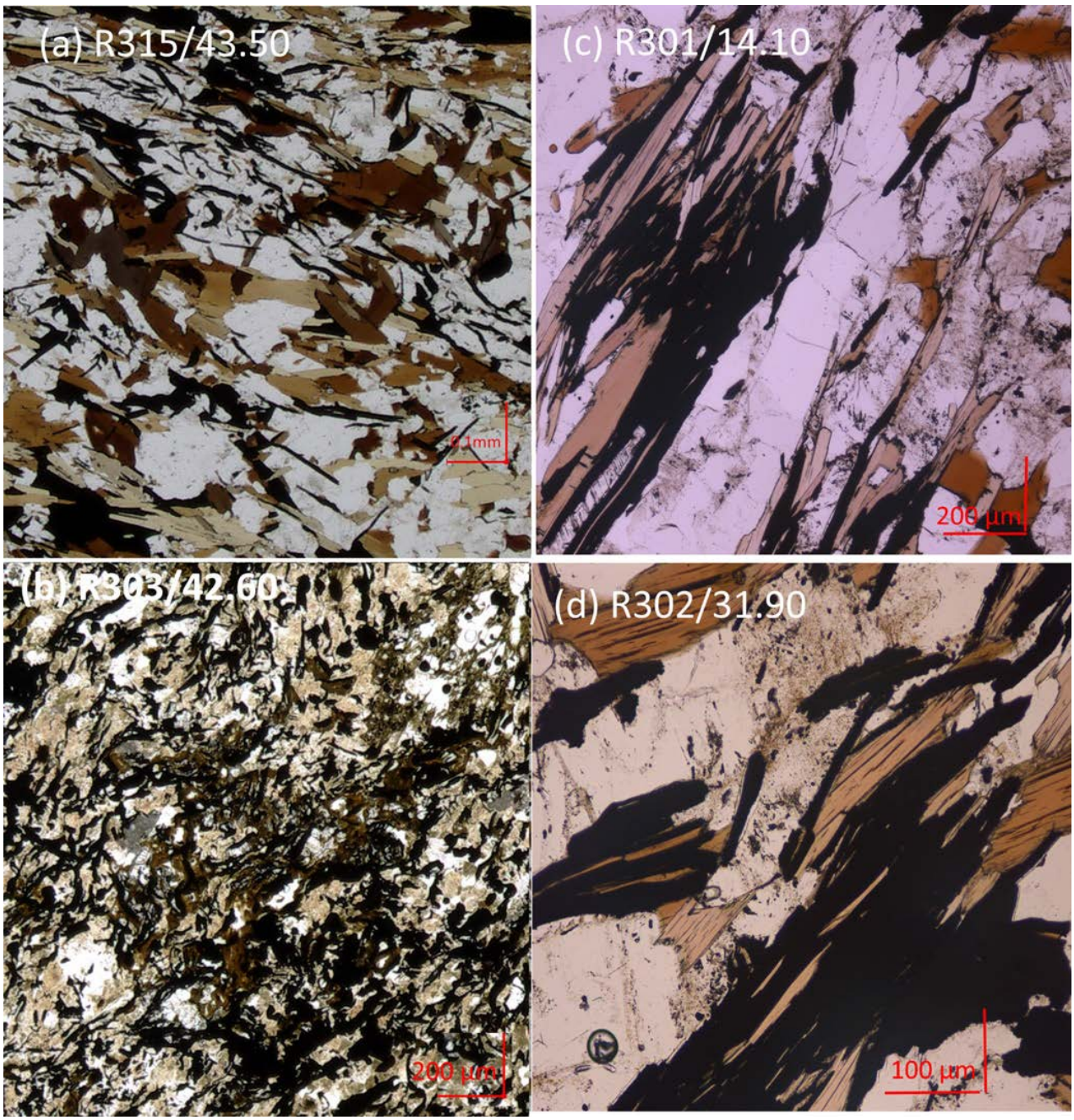

Fig. 19. Petrography of a graphite schist and gneiss from the Joutsijärvi area, large graphite flakes (500 to ≥1.5 mm) occurring as flat, plate-like crystals in the strongly foliated schist consisting of alternating biotite, quartz, plagioclase and chlorite.

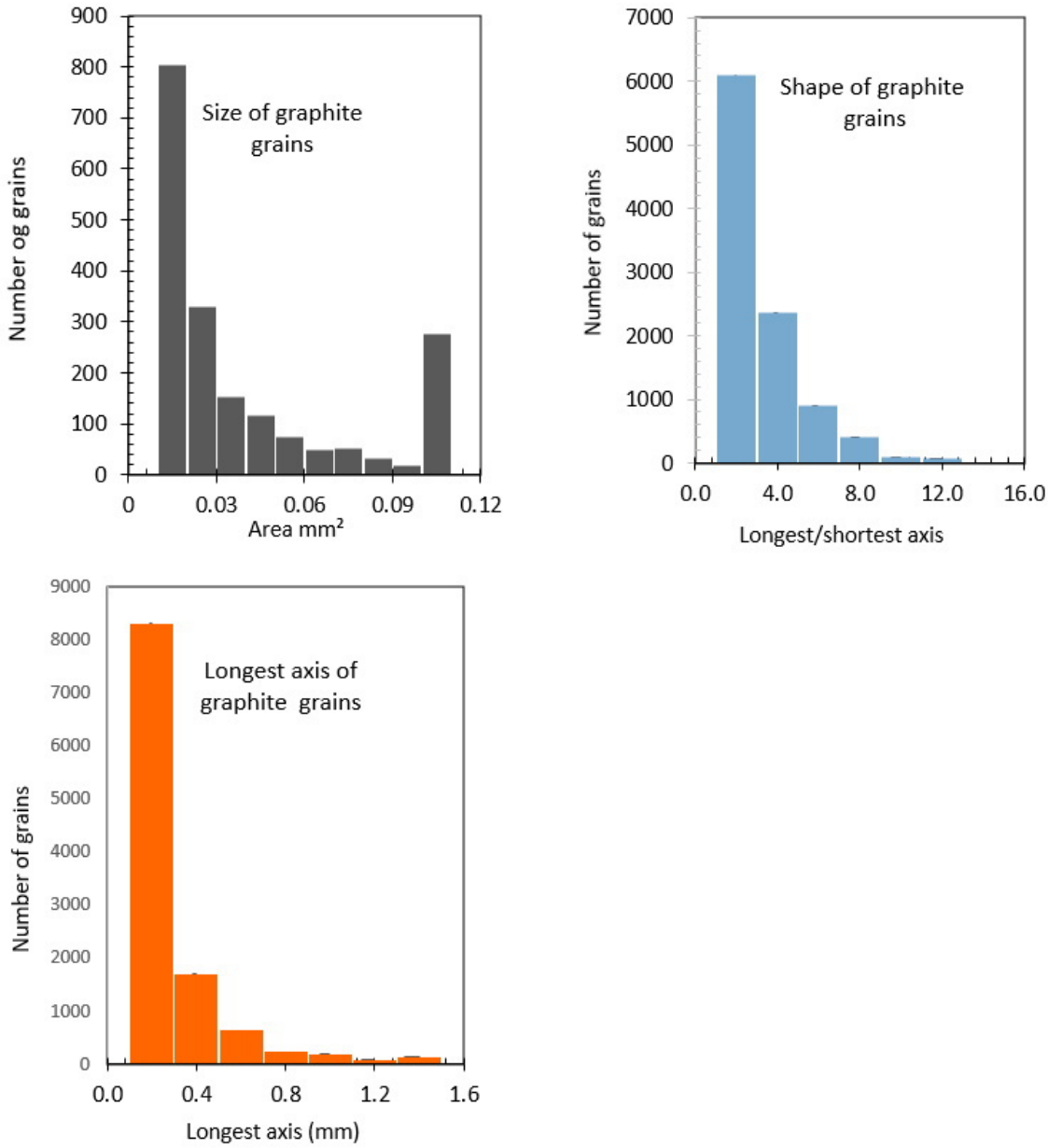

Fig. 20. Histograms showing the morphological variation of the graphite grains in several thin sections. Data were collected by digital microscopy| EM elemental analysis | KEYENCE VHX-7000N image analysis. The data are aggregate measurements of several thin sections and are believed to be representative Joutsijärvi graphite flakes.

The XRD method was employed to estimate the metamorphic crystallization temperatures recorded by graphite in the Kuusivaara–Joutsijärvi samples. The relationship between interplanar spacing, , $\mathbf{d}_{(002)}$, and crystallite size, $LC_{(002)}$ in accordance with Tagiri & Oba (1986), suggests that the studied graphite samples were classified as a fully ordered graphite phase (Fig. 21a). The graphitization degree (GD) was calculated using Equation 1 from Tagiri (1981), where, $\mathbf{d}_{(002)}$ is the interplanar spacing:

$$GD = \left[\frac{d_{(002)} - 3.7}{\log\left(\frac{LC_{(002)}}{1000}\right)}\right] \times 100 \quad (1).$$

Additionally, Equation 2 from Wada et al. (1994) was used to calculate the metamorphism temperature:

$$T(°C) = 3.2 \times GD + 280 \quad (2)$$

The average temperature found for Kuusivaara–Joutsijärvi samples clusters around 520 °C and 830 °C (Fig. 21b), with an average of 650 °C ± 100 °C. The results agree with the available geothermometric data for the terrain. The present study extends the idea that graphite crystallization is always a progressive reconstruction process, even to the highest grades of metamorphism. It is an irreversible phenomenon with the potential to be used as a metamorphic thermometer to assess the peak metamorphic temperature.

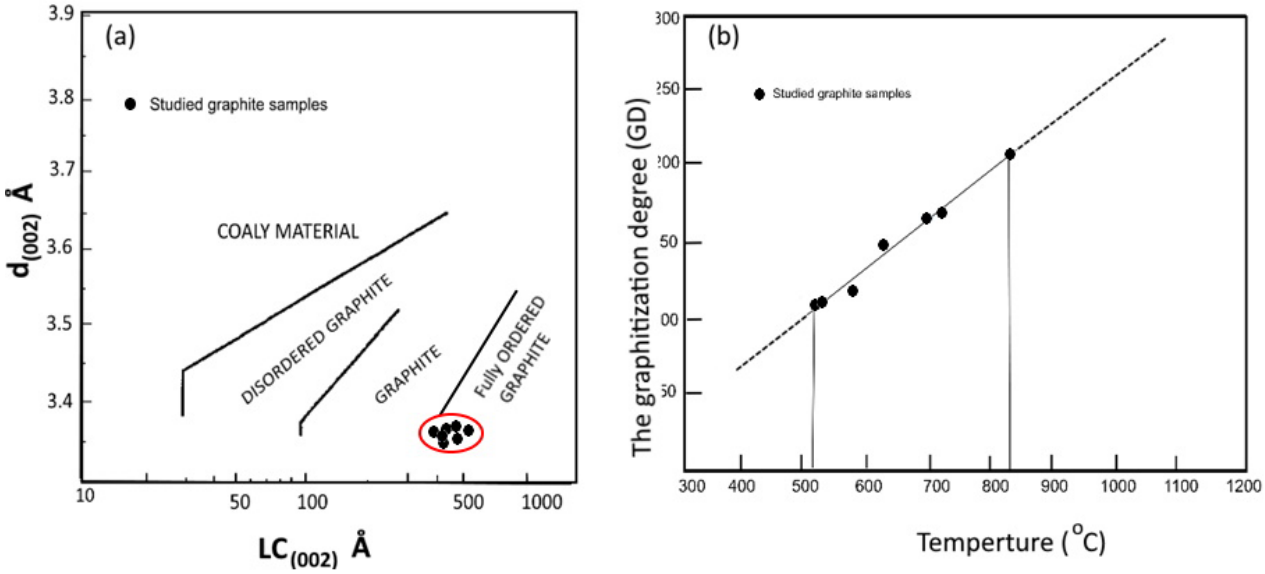

Fig. 21. a) Interplanar spacing d002 versus crystallite size Lc002 (Tagiri & Oba 1986). All samples are classified as fully ordered graphite. b) Graphitization degree (GD) versus X-ray diffraction data temperature (Wada et al. 1994). The derived temperatures for the studied graphite fall between 520 °C and 830 °C.

6.3.2 Geochemistry

The concentration of major oxides in the studied graphite-bearing samples displays remarkably large variation (see Table 6 and Fig. 22). In the box-and-whisker plot (Fig. 22a), constructed with major elements analysed by XRF and trace elements by ICP-MS, the carbon content varies from 2.31 to 32.10 wt%. The highest carbon content is seen in sample R315/43.50-43.55, while in sample R307/22.0-22.05, graphitic carbon remains at much lower levels. Sulphur contents in the studied graphite-bearing samples range from 1.40 to 27.80 wt%. Virtually all sulphur is distributed in iron sulphides (pyrite and pyrrhotite), as other sulphides are rare and occur only sporadically.

Silica has the highest concentration, ranging from 11.50 to 76.14 wt% SiO_2, followed by iron, ranging from 4.60 to 60.0 wt% Fe_2O_3. The percentage of Al_2O_3, with a range of 2.72 to 19.80 wt%, exceeds that found in biotite, feldspar and plagioclases. Na_2O and K_2O display variable or inverse relationships but relatively high concentrations, ranging from 0.2 to 4.64 wt% and 1.5 to 4.85 wt%, respectively. Na2O and K2O indicate the presence of sodic feldspar (albite) and K-feldspar, respectively. The MgO content ranges from 1.77 to 4.77 wt% and correlates with K2O, indicating the presence of magnesium-bearing minerals (chlorite, biotite) and muscovite.

Figure 22b displays the mineralogical composition of the graphite-bearing samples in a box-and-whisker plot. The mineral proportions of the whole rock major elements were calculated using the MINSQ program (Herrmann & Berry 2002), showing a low symmetry distribution of data. The most significant differences are observed in the major constituents: quartz, chlorite, pyrite and K-feldspar, followed by graphite, biotite and plagioclase. The range in the respective mineral values is also distinctly higher than in the other classes, such as mainly quartz (2.2–70.3 wt%), chlorite (4.2–42.5 wt%), pyrite (2.9–55.3 wt%), K-feldspar (0.5–24.2 wt%), biotite (5.8–15.8 wt%), plagioclase (0.4– 32.5 wt%) and graphite (2.3–38.2 wt%), followed by muscovite, calcite, and so on.

Table 6. Chemical results of major elements (wt.%) and graphite content (C_{gr}) from representative graphite-bearing samples from Joutsijärvi–Kuusivaara.

Sample	SiO_2	TiO_2	Al_2O_3	Fe_2O_3	MnO	MgO	CaO	Na_2O	K_2O	P_2O_5	S	C
R301/14.10-14.15	34.90	0.91	19.80	22.00	0.02	3.00	0.11	0.18	3.59	0.01	8.73	9.15
R302/31.90-31.95	26.20	1.10	10.30	40.00	0.03	4.62	0.15	0.34	2.65	0.01	7.52	5.88
R305/20.80-20.85	11.50	0.51	5.36	60.00	0.02	2.15	0.03	0.28	1.85	0.01	27.80	5.61
R306/49.15-49.20	32.10	1.20	12.70	30.00	0.01	2.18	0.67	1.44	2.10	0.04	14.10	11.50
R314/6.55-8.20	61.89	0.70	5.01	13.76	0.04	3.32	0.02	0.07	2.69	0.01	4.24	6.94
R314/9.85-11.05	66.51	0.89	5.52	9.75	0.05	3.86	0.03	0.08	3.05	0.01	2.23	6.73
R314/23.10-25.50	54.38	0.69	4.89	19.15	0.03	2.99	0.02	0.08	2.42	0.01	6.41	7.6
R314/24.00-24.05	51.20	0.64	15.40	4.60	0.02	1.97	3.48	4.64	1.40	0.56	1.69	12.50
R314/25.50-27.65	56.97	0.64	4.87	16.72	0.03	2.82	0.03	0.07	2.25	0.01	5.87	8.39
R314/27.65-28.80	69.22	0.46	3.36	12.25	0.02	1.97	0.03	0.09	1.60	0.01	4.08	5.59
R314/31.40-33.80	46.40	0.44	4.74	27.44	0.03	2.19	0.03	0.07	1.81	0.01	9.81	5.7
R314/39.00-40.45	55.03	0.56	4.02	19.72	0.03	2.17	0.03	0.08	1.99	0.01	6.73	8.31
R314/43.40-45.00	27.70	0.67	4.31	31.72	0.04	2.42	0.03	0.05	2.31	0.01	17.00	12.4
R314/45.00-46.80	36.08	0.52	3.33	33.87	0.03	1.84	0.01	0.05	1.82	0.01	10.20	10.9
R314/46.80-48.20	38.12	0.60	4.06	29.44	0.04	2.29	0.01	0.05	2.14	0.01	10.80	11.1
R314/52.35-53.70	47.07	0.50	4.02	27.87	0.03	2.22	0.04	0.07	1.93	0.02	10.00	4.9
R315/43.50-43.55	40.70	0.53	7.12	4.60	0.01	1.77	0.95	1.57	1.35	0.03	1.53	32.10
R315/ 67.90-69.40	58.84	0.66	3.72	21.58	0.04	1.99	0.84	0.13	1.78	0.41	7.29	7.29
R316/46.80-46.85	29.30	1.44	13.20	28.00	0.07	4.77	0.62	1.25	4.85	0.02	8.28	8.41
R320/22.90-22.95	35.80	0.46	9.95	32.00	0.01	2.18	0.14	0.79	2.75	0.05	14.50	8.69

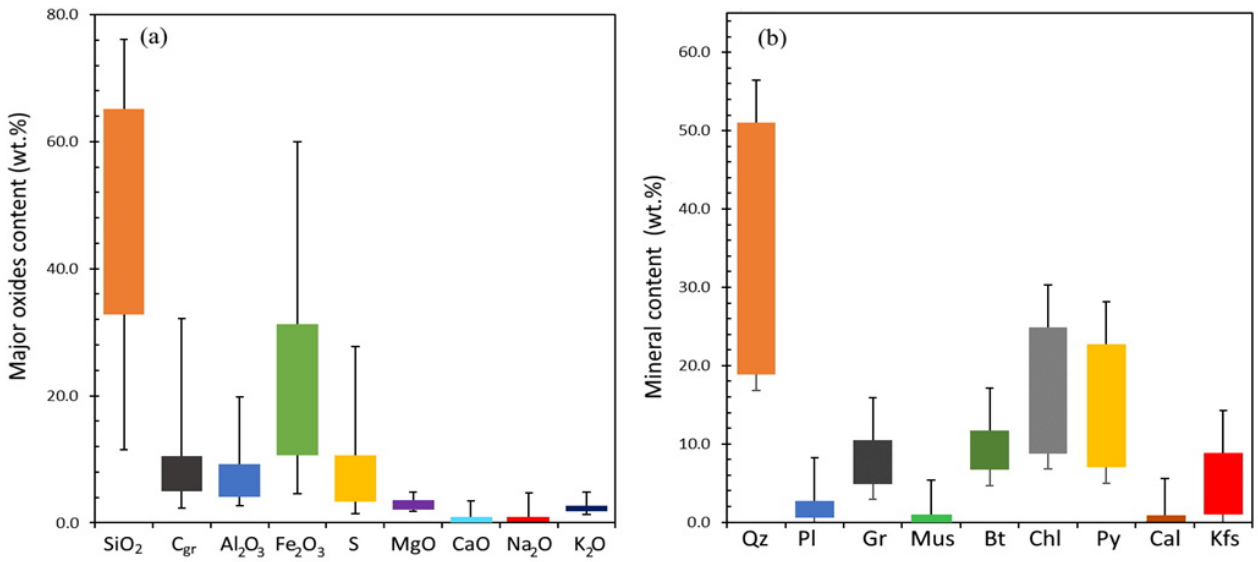

Fig. 22. Chemical composition of the graphite-bearing rocks in the Kuusivaara–Joutsijärvi area. a) Box-and-whisker plot for the major oxides. b) Mineralogical phases in the graphite-rich samples (>5 wt% C_{gr}). (Qz = quartz, Pl = plagioclase, Gr = graphite, Mus = muscovite, Bt = biotite, Chl = chlorite, Py = pyrite, Cal = calcite, Kfs = K-feldspar).

7 GRAPHITE BENEFICIATION

Graphite-bearing rocks from Rautalampi–Käpysuo and Raisjoki–Emas were beneficiated by flotation to improve their quality. The graphite ore beneficiation involved several stages, including ore crushing, grinding, flotation and graphite purification (alkaline roasting and sulphuric acid leaching). A forty-metre length of composite drill core sample was divided into 700-g subsamples for flotation testing at GTK Mintec, Mineral Processing Pilot Plant, at Outokumpu (Table 7). The samples were prepared by crushing and sieving to <1.4 mm (<250 µm). The d80 of the flotation feed samples was approximately 43 µm. Several stages of flotation are essential to produce clean graphite concentrates of 85–90% C with recoveries between 67% and 83% for Rautalampi–Käypysuo and 87–89% C with recoveries between 48% and 66% for Raisjoki–Emas (Fig. 23). The particle-size distribution for Käpysuo concentrate and Raisjoki should be added to examine whether there are any differences between the products of these ores (flake type and black schist). After alkaline roasting with NaOH at 500 °C, and followed by water washing and H2SO4 leaching, the fine flotation concentrates from Käpysuo and Raisjoki ores can be purified to about 99.4% and >99.0%, respectively. Furthermore, with a high-grade graphite feed, the NaOH consumption can be reduced and the product purity can be further improved.

SEM images show the impurity minerals scattered in graphite flakes, including large ones that exist independently in the shape of clouds, and small particles of impurities adhering to the surface of graphite scales (Fig. 24). Combined with EDS images analyses, these impurities stacked on the flake graphite layer and adhering to the flake graphite layer interlayer are composed of Si, Al, Fe, Mg, Na, K and Ca. These impurities must be removed to improve the purity of graphite in the purification process.

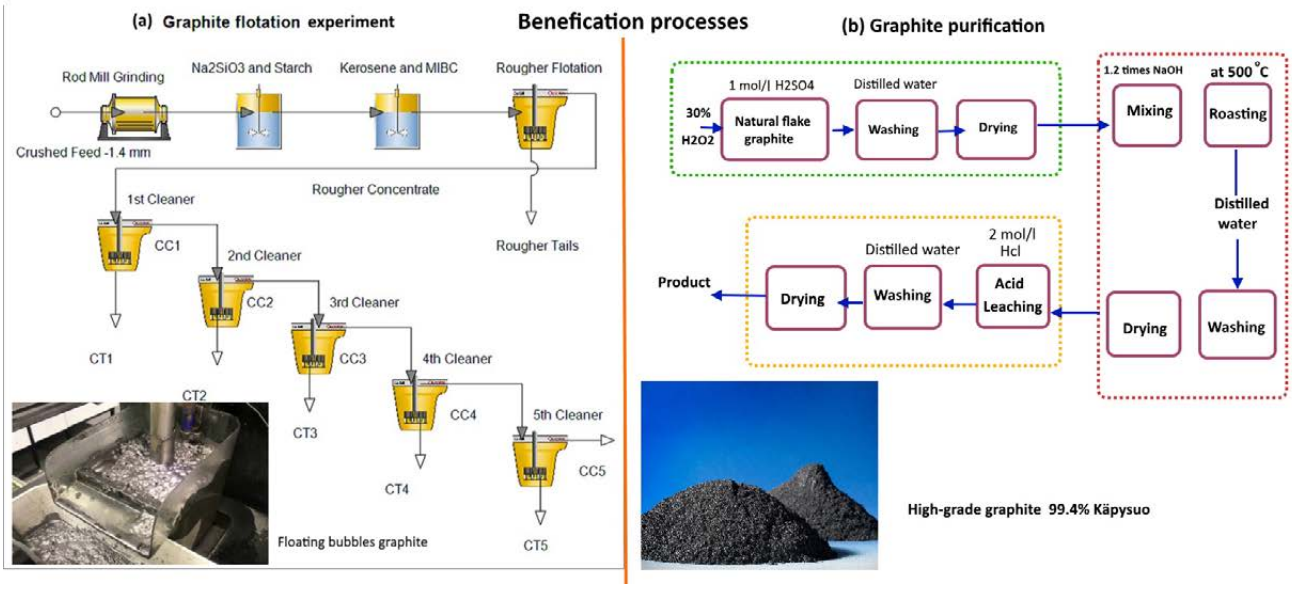

Fig. 23. Flake graphite upgrading processes at GTK Mintec, Outokumpu.

Table 7. Samples selected for mineralogical and beneficiation processes, Käpysuo graphite ore.

Drill core samples	Depth range (m)	Lengths of core	Crushed sample	Thin section	Lithology	FC %
		required (m)	weight (Kg)			
N4442017R2	62.85-64.85	2		64.8	Graphite gneiss	7.9
N4442017R2	64.85-66.85	2		66.8	Graphite gneiss	12.6
N4442017R2	66.85-68.85	2		74	Black schist	18.9
N4442017R2	68.85-70.85	2		70.8	Graphite gneiss	12.2
N4442017R2	70.85-72.85	2		72.8	Graphite gneiss	8.2
N4442017R2	72.85-74.60	1.75		74.6	Graphite gneiss	19.6
N4442017R2	74.60-75.70	1.1		75.7	Graphite gneiss	6.8
Total		12.85				
N4442017R7	102-55-104.60	2.05		102.5	Black schist	12.2
N4442017R7	104.60-106.60	2.06		104.6	Black schist	6.3
N4442017R7	106.60-108.60	2		106.6	Graphite gneiss/Black schist	9.4
N4442017R7	108.60-111.00	2.4		108.6	Graphite gneiss	5.8
N4442017R7	111.00-113.45	2.45		111	Graphite gneiss	10.2
Total		10.96		-		
RTL/PH-16	229.1-231.85	2.75	2.7		Black schist	13.5
RTL/PH-16	231.85-234.65	2.8	0.9	232.95	Black schist	17.9
RTL/PH-16	234.65-237.40	2.75	2.4		Graphite gneiss/Black schist	8.5
RTL/PH-16	237.40-240.05	2.65	1.5	235	Graphite gneisses/Black schist	5.2
Total		10.95	7.5			
RTL/PH-17	159.55-161.55	2	2		Graphite gneiss	5.5
RTL/PH-17	161.55-163.55	2	1.7	161.8	Graphite gneiss	9.7
RTL/PH-17	163.55-166.55	2	1.5	163	Graphite gneiss	8.9
RTL/PH-17	166.55-167.95	2.4	1.6		Graphite gneiss	14.2
Total		8.4	6.8	-		

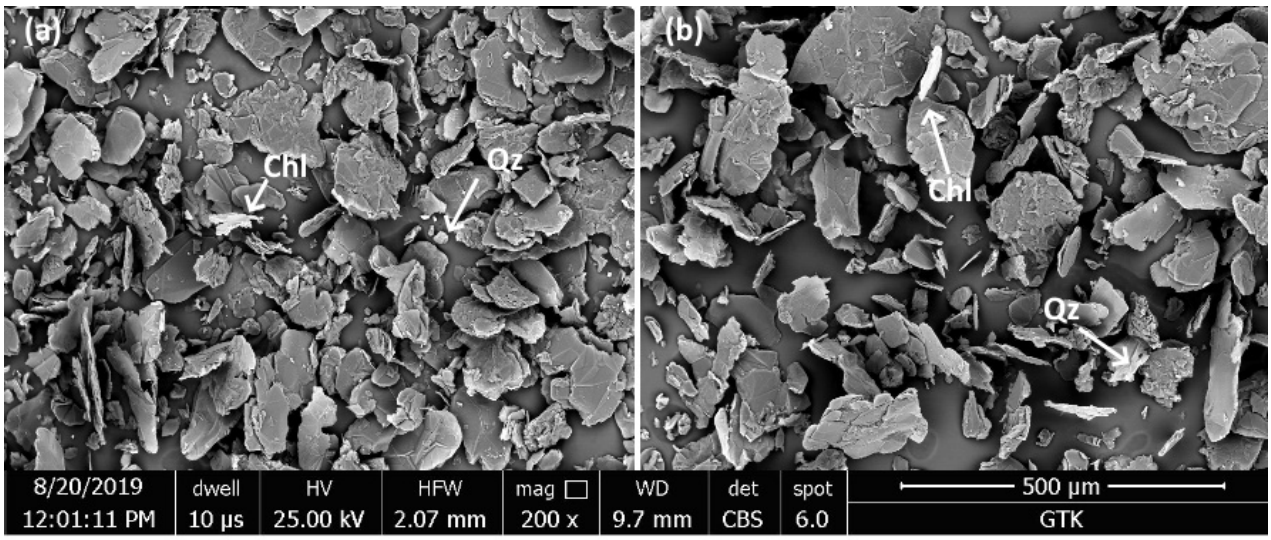

Fig. 24. Scanning electron microscopy (SEM) images showing the microstructure of graphite flakes after beneficiation processes at a low magnification and the highest magnification. Impurity minerals are scattered on the graphite flakes.

8 DISCUSSION

Geologically, Finnish bedrocks are highly favourable for the formation of flake graphite deposits. To evaluate the known graphite occurrences and their potential, detailed geophysics, petrographic, mineralogical, geochemical and graphite concentrate results are presented. It is clear from the analytical results presented here that the graphite flakes mainly occur in black schist and mica gneiss rocks, which covered most of the studied samples in the Käpysuo, Raisjoki and Joutsijärvi areas.

The graphite is characterized by many parameters, the two most important ones for commercially traded flake graphite being the flake-size distribution and carbon content (purity). Characterization of the size and morphology of the graphite flakes is therefore important in ore evaluation. Flake-size measurements from several thin sections using digital microscopic and SEM methods are usually necessary to provide a statistically significant description of the flake-size distribution. Graphite flakes range in size from fine flakes (<150 µm), such as in Raisjoki–Emas, to medium flakes (150–400 µm) and coarse flakes (400–1600 µm), such as in the Rautalampi–Käypysuo and Joutsijärvi samples. An example of the result of such measurements is presented in Figure 25, which shows aggregate grain morphological measurements of graphite particles in the examined samples.

Beneficiation using multi-stage grinding and flotation processes was conducted to increase the graphite grade from 55% to 90% fixed carbon (FC) with recovery ranges between 67% and 83% for Käypysuo and to 87–89% C with recoveries between 48–66% for Raisjoki–Emas. The flotation results indicated that the graphite concentrate still contains some mineral impurities, making it difficult to purify using only the typical flotation technique. Quartz and sulphides comprised most of the impurity minerals in the investigated graphite ore. Alkaline roasting and acid leaching processes were used to prepare high-purity graphite from fine graphite concentrate. The results demonstrated that the graphite grade of Käypysuo ore can be increased to a high-purity graphite (99.4% FC) by grinding to an exceedingly small particle size of <30 µm, and it can therefore be possible to achieve the requirements for lithium-ion battery production. Although the Raisjoki–Emas graphite was characterized by small-sized graphite flakes, purification using the alkaline roasting process increased the graphite purity to higher than 99% FC.

Based on the major element variations presented above, the graphite-bearing rocks from the studied areas are primarily composed of tholeiitic basalt to calc-alkaline rocks. The AFM diagram (Irvine & Barager 1971) suggested that the studied graphite-

bearing rocks from Raisjoki–Emas and Joutsijärvi samples define an Fe-rich tholeiitic affinity, whereas the rocks of the Rautalampi–Käpysuo samples have a lower Fe content and thus calc alkaline rather than tholeiitic affinities (Fig. 25a). In discrimination Jensen diagram (Fig. 25b), the studied graphite-bearing rocks also define slightly separate tholeiitic/calc–alkaline trends, suggesting at least three major geochemical groups within studied metavolcanic rocks: (i) calc–alkaline schists (andesites–dacites), (ii) tholeiitic basalts–basaltic andesites and (iii) a high-Fe tholeiite basalt field.

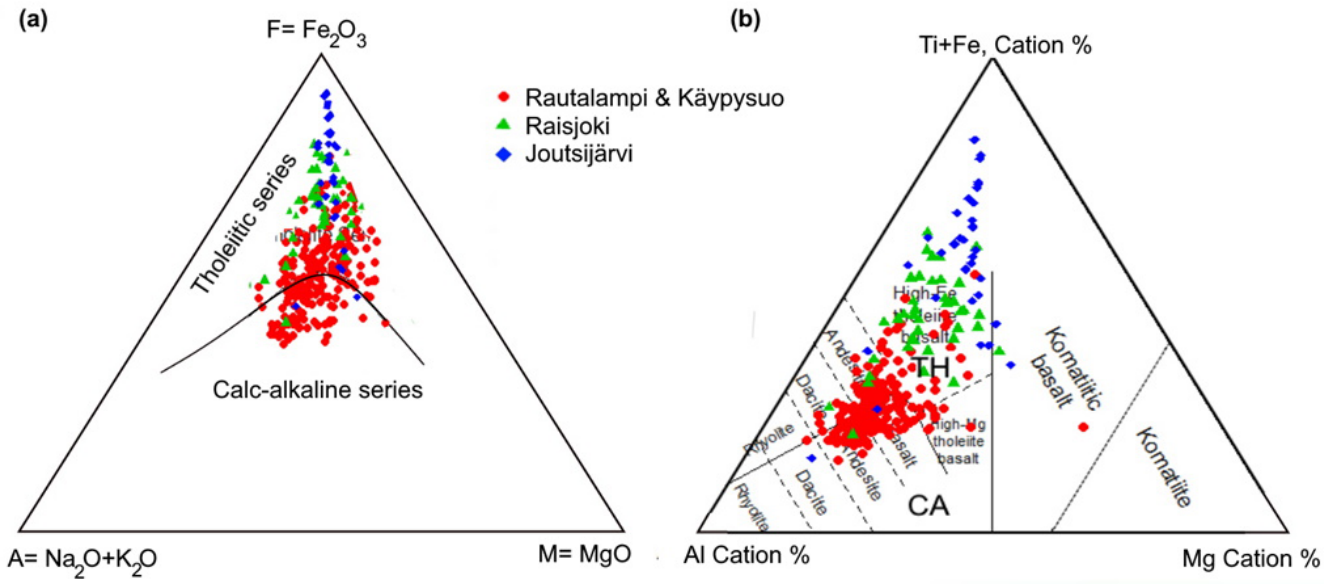

Fig. 25. Compositional diagrams showing the chemistry of graphite-bearing rocks. a) An AFM diagram for the forearc bodies ($A=Na_2O+K_2O$, $F=FeO+Fe_2O_3$, $M=MgO$) that differentiates between tholeiitic and calc-alkaline rocks (Irvine & Baragar 1971). b) Discrimination between calc-alkalic, tholeiitic and komatiitic igneous rocks (Jensen 1976).

9 CONCLUSIONS

During several GTK graphite exploration projects, e.g., the Green Minerals Project (2018–2020), the Battery Mineral Project (2016–2019 & 2019–2022) and BatCircle 1.0 & 2.0 (2019–2020, 2021–2024), multiple areas with potential for flake graphite occurrences having a high metamorphic grade have been discovered in Finland.

The studied flake graphite in the Käpysuo, Raisjoki–Emas and Joutsijärvi occurrences have typically formed as a result of metamorphic (regional or contact) accumulations of organic matter in the ore-bearing rock, which are composed of black schist, mica–quartz gneiss and amphibolite.

Two main variables determining the product type and the end application of flake graphite are its flake size, and purity. Graphite flakes in the Käpysuo and Joutsijärvi targets ranged in size from medium flakes (150–400 µm) to coarse flakes (400–1600 µm in length), in contrast to the fine graphite flakes (<150 µm) in the Raisjoki target.

The physical purification method of flotation was not able provide sufficient purity enhancement for the studied graphite samples. This may be due to the impurities present as sulphides, chlorite and quartz in trace levels intercalated in the crystal structure. However, several stages of flotation were successful and provided adequate purity enhancement to between 85–90% C with recoveries between 67% and 83% for Rautalampi–Käypysuo and between 87–89% C with recoveries between 48% and 66% for Raisjoki–Emas. Moreover, alkaline roasting and acid leaching were able to enhance the purity to over 99% carbon content for both Käpysuo (99.4% C) and Raisjoki (>99.0% C) samples.

REFERENCES

Al-Ani, T. & Sarapää, O. 2016. Mineralogy and geochemistry of flake graphite occurrences in Joutsijärvi, Northern Finland. Geological Survey of Finland, archive report 55/2016. 39 p. Available at: https://tupa.gtk.fi/raportti/arkisto/55_2016.pdf

Al-Ani, T., Ahtola, T., Cutts, K. & Torppa, A. 2022. Metamorphic evolution of graphite in the Paleoproterozoic Savo Schist Belt (SSB), Central Finland: Constraints from geothermetric modeling. Ore Geology Reviews 141, p. 104672. Available at: https://doi.org/10.1016/j.oregeorev.2021.104672

Al-Ani, T., Ahtola, T. & Kuusela, J. 2018. Prospecting and exploration of flake graphite occurrences in Central and Southern Finland. Geological Survey of Finland, Open File Work Report 24/2018. 25 p. Available at: https://tupa.gtk.fi/raportti/arkisto/24_2018.pdf

Al-Ani, T., Leinonen, S. & Ahtola, T. 2019. Mineralogy and Petrography of High-quality flake graphite rocks. Luopioinen, Pihtipudas and Seinäjoki, Southern and Central Finland. Geological survey of Finland, Open File Report. 36 p.

Al-Ani, T., Leinonen, S., Ahtola, T. & Salvador, D. 2020. High-grade flake graphite deposits in metamorphic Schist Belt, Central Finland – Mineralogy and beneficiation of graphite for lithium-ion battery applications. Minerals 10(8), p. 680. Available at: https://www.mdpi.com/784178

Al-Ani, T., Sarapää, O. & Lintinen, P. 2016. Mineralogy, petrography and geochemistry of Venejärvi, Tervola, Rytijänkä and Jaurujoki graphite schists and gneisses in Northern Finland. Geological Survey of Finland, archive report 54/2016. 17 p. Available at: https://tupa.gtk.fi/raportti/arkisto/54_2016.pdf

Alviola, R. & Nurmela, P. 1994. Tutkimustyöselostus Luopioisten kunnassa, valtausalueella Niinimetsä 1, kaiv. rek. n:o 4701/1, suoritetuista tutkimuksista. Geological Survey of Finland, claim report M06/2132/-94/1/81. 11 p., 18 app. pages. (in Finnish). Available at: https://tupa.gtk.fi/raportti/valtaus/m06_2132_94_1_81.pdf

Aoya, M., Kouketsu, Y., Endo, S., Shimizu, H., Mizukami, T., Nakamura, D. & Wallis, S. 2010. Extending the applicability of the Raman carbonaceous-material geothermometer using data from contact metamorphic rocks. J. Metamorph. Geol. 28 (9), 895–914. Available at: https://onlinelibrary.wiley.com/doi/10.1111/j.1525-1314.2010.00896.x

Arkimaa, H., Hyvönen, E., Lerssi, J., Loukola-Ruskeeniemi, K. & Vanne, J. 2000. Proterozoic black shale formations and aeromagnetic anomalies in Finland, 1:1000000. Geological Survey of Finland, Special Maps 45.

Aurola, E. 1965. Selostus Merijärvellä suoritetuista grafiittitutkimuksista, Geological Survey of Finland, archive report M17/Mj-65/1/81. 18 p., 47 app. pages. (in Finnish). Available at: https://tupa.gtk.fi/raportti/arkisto/m17_mj_65_1_81.pdf

Bedrock of Finland – DigiKP. Digital map database [Electronic resource]. Espoo: Geological Survey of Finland. [referred 16.11.2023]. Version 2.0.

Beowulf Mining 2022. Aitolampi – Graphite. Available at: https://beowulfmining.com/projects/finland/aitolampi/#overview. [Retrieved 14 March 2022]

Beyssac, O., Goffé, B., Chopin, C. & Rouzaud, J. N. 2002. Raman spectra of carbonaceous material in metasediments: a new geothermometer. Journal of metamorphic Geology 20(9), 859–871.

Eerola, T. 2022. Corporate conduct, commodity, and place: Ongoing mining and mineral exploration disputes in Finland and their implications for the social license to operate. Resources Policy 76, 102568. Available at: https://doi.org/10.1016/j.resourpol.2022.102568

European Commission 2018. Report on Raw Materials for Battery Applications. SWD (2018) 245/2 Final. Available at: https://data.consilium.europa.eu/doc/document/ST-9179-2018-REV-1/en/pdf

García-Casco, A., Torres Roldán, R. L., Millán Trujillo, G., Monié, P. & Haissen, F. 2001. High-grade metamorphism and hydrous melting of metapelites in the Pinos Terrane (W Cuba): Evidence for crustal thickening and extension in the northern Caribbean collisional belt. Journal of Metamorphic Geology, Vol. 19, 699–715. Available at: https://onlinelibrary.wiley.com/doi/10.1046/j.0263-4929.2001.00343.x

Hautaniemi, H., Kurimo, M., Multala, J., Leväniemi, H. & Vironmäki, J. 2005. The 'three in one' aerogeophysical concept of GTK in 2004. In: Airo, M.-L. (ed.) Aerogeophysics in Finland 1972–2004: Methods, System Characteristics and Applications. Geological Survey of Finland, Special Paper 39, 21–74. Available at: https://tupa.gtk.fi/julkaisu/specialpaper/sp_039_pages_021_074.pdf

Henry, D. J. 1981. Sulfide-silicate relations of the staurolite grade pelitic schists, Rangeley quadrangle, Maine. The University of Wisconsin-Madison.

Henry, D., Guidotti, C. & Thomson, J. 2005. The Ti-Saturation Surface for Low-to-Medium Pressure Metapelitic Biotites: Implications for Geothermometry and Ti-Substitution Mechanism. American Mineralogist 90, 316–328. Available at: https://doi.org/10.2138/am.2005.1498

Herrmann, W. & Berry, F. 2002. MINSQ – a least squares spreadsheet method for calculating mineral proportions from whole rock major element analyses. Geochemistry Exploration Environment Analysis 2(4), 361–368. Available at: https://doi.org/10.1144/1467-787302-010

Holdaway, M. J. 2000. Application of new experimental and garnet Margules data to the garnet-biotite geothermometer. American mineralogist 85(7–8), 881–892. Available at: https://doi.org/10.2138/am-2000-0701

Irvine, T. N. & Baragar, W. R. A. 1971. A guide to the chemical classification of the common volcanic rocks. Can. J. Earth Sci. 8, 523–548.

Isomaa, J. 1991. Tutkimustyöselostus Inarin kunnassa valtausalueella Lutto 1. kaiv. rek. 4637/1 suoritetuista tutkimuksista vuonna 1989. Geological Survey of Finland, claim report M06/3831/-91/1/10. 2 p., 2 app. pages. (in Finnish). Available at: https://tupa.gtk.fi/raportti/valtaus/m06_3831_91_1_10.pdf

Isomaa, J. 1993. Tutkimustyöselostus Kuttura-Saariselkäalueen grafiittiaiheiden tutkimuksista Inarin ja Sodankylän kunnissa. Geological Survey of Finland, archive report M19/3831/-93/1/81. 6 p., 3 app. pages. (in Finnish). Available at: https://tupa.gtk.fi/raportti/arkisto/m19_3831_93_1_81.pdf

Jensen, L. S. 1976. A new cation plot for classifying subalkalic volcanic rocks. Ontario Division of Mines, MP, Vol. 66., p. 22.

Kuusela, J., Nygård, H., Salvador, D., Al-Ani, T., Kujasalo, J. P., Leväniemi, H., Thurman, N., Hulkki, H., Taivalkoski, A., Lehto, T. & Kuva, J. 2022. Indications of flake graphite and Ni–Co–Au mineralization in metavolcanic sequences in Emas, Kruunupyy, western Finland. Geological Survey of Finland, Open File Research Report 44/2022. 43 p., 4 app. pages. Available at: https://tupa.gtk.fi/raportti/arkisto/44_2022.pdf

Kuusela, J., Salvador, D., Nurkkala, J., Heilimo, E., Nousiainen, M., Ahtola, T. & Al-Ani, T. 2021. The Vaajasalmi flake graphite, Rautalampi, Central Finland. Geological Survey of Finland, Open File Research Report 60/2021. 34 p., 7 app. pages. Available at: https://tupa.gtk.fi/raportti/arkisto/60_2021.pdf

Laitakari, A. 1925. Die Graphitvorkommen in Finnland und ihre Entstehung. Geological Survey of Finland, Geotechnical publications 40. 100 p., 2 app. pages. (in German). Available at: https://tupa.gtk.fi/julkaisu/geoteknillinen/gt_s_040.pdf

Leino, J. & Miettinen, E. 2020. Mineral exploration, acceptance, and possibilities of participation – The case of Heinävesi mineral exploration conflict. Ympäristöoikeuden vuosikirja XIII, 265–367. (in Finnish)

Mattila, H. 1978. Saarenputaan ja Juurakkajärven grafiitti-Cu-kriittisten sähköanimaloiden tutkimukset v. 1977. Rautaruukki Oy, report OKU_4273. 11 p., 13 app. pages. (in Finnish). Available at: https://tupa.gtk.fi/raportti/arkisto/ro_10_78.pdf

Nuutilainen, J. 1968. On the geology of the Misi Iron Ore Province, Northern Finland. Annales Academiae Scientiarum Fennicae, Series A. III. Geologica–Geographica. 98 p.

Palosaari, J. 2021. Flake graphite prospects in the Fennoscandian Shield. Licentiate thesis, Åbo Akademi University. 50 p. Available at: https://urn.fi/URN:NBN:fi-fe2021060835779

Palosaari, J., Latonen, R. M., Smått, J. H., Blomqvist, R. & Eklund, O. 2016. High-quality flake graphite occurrences in a high-grade metamorphic region in Sortland, Vesterålen, northern Norway. Nor. J. Geol. 96, 19–26. Available at: http://dx.doi.org/10.17850/njg96-1-03

Pankka, H. 1999. Tutkimustyöselostus Kemijärven kunnassa valtausalueilla Kuusivaara 1 kaiv.rek.n:o 6157/1 ja Aapalampi 1-2 kaiv.rek.n:o 6158/1-2 suoritetuista tutkimuksista. Geological Survey of Finland, claim report M06/3632,3634/-99/1/10. 6 p., 4 app. pages. (in Finnish). Available at: https://tupa.gtk.fi/raportti/valtaus/m06_3632_3634_99_1_10.pdf

Pasteris, J. D. 1989. In situ analysis in geological thin sections by laser Raman microprobe spectroscopy: a cautionary note. Applied Spectroscopy 43(3), 567–570.

Puustinen, K. 2003. Suomen kaivosteollisuus ja mineraalisten raaka-aineiden tuotanto vuosina 1530–2001, historiallinen katsaus erityisesti tuotantolukujen valossa. Geological Survey of Finland, archive report M101/2003/3. 578 p. (in Finnish). Available at: https://tupa.gtk.fi/raportti/arkisto/m10_1_2003_3.pdf

Rahl, J. M., Anderson, K. M., Brandon, M. T. & Fassoulas, C. 2005. Raman spectroscopic carbonaceous material thermometry of low-grade metamorphic rocks: calibration and application to tectonic exhumation in Crete, Greece. Earth Planet Sci. Lett. 240, 339–354. Available at: https://doi.org/10.1016/j.epsl.2005.09.055

Sarapää, O. 1988. Grafiitti. In: Haapala, I. (ed.) Suomen teollisuusmineraalit ja teollisuuskivet. Helsinki: Yliopistopaino, 66–73. (in Finnish)

Sarapää, O. & Kukkonen, I. 1984. Grafiittitutkimukset Kiihtelysvaaran Hyypiässä vuosina 1981–1983. Geological Survey of Finland, archive report M81/4241/-84/2. 30 p., 15 app. pages. (in Finnish). Available at: https://tupa.gtk.fi/raportti/arkisto/m81_4241_84_2.pdf

Smulikowski, W., Desmons, J., Fettes, D., Harte, B., Sassi, F. & Schmid, D. 2007. Types, grade, and facies of metamorphism. In: Fettes, D. & Desmons, J. (eds) Metamorphic rocks: A Classification and Glossary of Terms. Recommendations of the Union Geology Sciences, Subcommission on the Systematics of metamorphic Rocks. Cambridge University Press, 16–23.

Tagiri, M. 1981. A measurement of graphitizing-degree by the X-ray powder diffractometer. J. Japan. Asoc. Mineral. Petrol. Econ. Geol., Vol. 76, 345–352.

Tagiri, M. & Oba, T. 1986. Hydrothermal synthesis of graphite from bituminous coal at 0.5-5.0 kbar water vapor pressure and 300-600°C. J. Japan. Asoc. Mineral. Petrol. Econ. Geol., Vol. 81, 260-271.

Wada, I. H., Tomita, T., Iuchi, K., Ito, M. & Morikiyo, T. 1994. Graphitization of carbonaceous matter during metamorphism with reference to carbonate and pelitic rocks of contact and regional metamorphism, Japan. Contrib. Mineral. Petrol., Vol. 118, 217–228.

Won, I. J., Keiswetter, D. A., Fields, G. R. A. & Sutton, L. C. 1996. GEM-2: A new Multifrequency Electromagnetic Sensor. JEEG, Vol. 1, Issue 2, August 1996, 129–137.

Zen, E. 1981. Metamorphic Mineral Assemblages of Slightly Calcic Pelitic Rocks in and around the Taconic Allochthon, Southwestern Massachusetts and Adjacent Connecticut and New York, United States. U.S. Geological Survey, Professional paper 1113. 128 p. Available at: https://doi.org/10.3133/pp1113

All GTK's publications online at hakku.gtk.fi